General and Comparative Endocrinology 278 (2019) 25–41

Contents lists available at ScienceDirect

General and Comparative Endocrinology

journal homepage: www.elsevier.com/locate/ygcen

Neuropeptide- and serotonin- cells in the brain of *Rhodnius prolixus* (Hemiptera) associated with the circadian clock

Xanthe Vafopoulou*, Martha Hindley-Smith, Colin G.H. Steel

Department of Biology, York University, Toronto, Canada

ARTICLE INFO

Keywords:
Pigment-dispersing factor
FMRFamide
Allatostatin
Crustacean cardioactive peptide
Lateral neurons
Accessory medulla

ABSTRACT

The neuronal pathways of the circadian clock in the brain of *R. prolixus* have been described in detail previously, but there is no information concerning the cells or their pathways which relay either inputs to the clock (e.g. for light entrainment), or outputs from it to driven rhythms. Here, we employ antisera to three neuropeptides (type A allatostatin-7, crustacean cardioactive peptide and FMRFamide), and serotonin in confocal laser scanning immunohistochemistry to analyze the distribution of cell bodies and their projections in relation to the principle circadian clock cells (lateral cells, LNs) for all four neuron types. LNs are revealed following labelling with anti-pigment dispersing factor in double labelled preparations. Regions of potential communication between ramifications of the LNs and each of the four other neuron types is described (identified by close superposition of their neurites in various brain regions), as is their detailed projections within the brain. Neuromodulation is sometimes suggested by close, but not intimate, proximity of varicosities of neurites. We infer that some neuron types comprise input pathways to the LNs, some are outputs to neuroendocrine or behavioral rhythms, and others participate in both input and output pathways, sometimes by the same neuron type but in different locations. For example, one retinula cell in each ommatidium is immunoreactive for allatostatin A; its axon projects to the medulla making superpositions with LNs, as do serotonin cells in the optic lobe, indicating roles of both neuron types in light input (entrainment) to the clock. But in other brain areas, these same types appear to mediate outputs from the clock. The accessory medulla has been widely reported as the principle center of integration in other insects; but we found sparse evidence of this in *R. prolixus* as it contains few neurites other than those from the clock cells. Rather, the importance of neural pathways involving the medulla and the superior protocerebrum is emphasized. We conclude that there is a vast and complex web of interactions in the brain with the LNs, which potentially receive multiple pathways of inputs and outputs that could drive rhythmicity in a multitude of downstream cells, rendering a host of output pathways rhythmic, notably hormone release from neurosecretory cells and behaviors.

1. Introduction

Circadian clocks are essential for the generation of circadian rhythms that mediate temporal organization within an organism. This organization is crucial, not only for the coordination of all physiological functions in an organism, but to maintenance of life itself (reviews by Golombek and Rosenstein, 2010; Pittendrigh, 1993). Insects have played a pivotal role in the development of the underlying concepts, particularly in relation to the regulation of physiology and behavior (reviews by Allada and Chung, 2010; Helfrich-Förster, 2018; Tomioka, 2014). In insects, the molecular mechanism by which specialized cells (clock cells) generate these circadian rhythms has been extensively

Abbreviations: Nomenclature for regions of the insect brain, and abbreviations for them, are according to those introduced by Ito et al. (2014). Orientations of all images are relative to the *body axis*. AME, accessory medulla; b-anterior, anterior of the longitudinal axis of the body; AstA, allatostatin A; DNs, dorsal neurons; IR, immunoreactivity; LA, lamina; LNs, lateral neurons; LO, lobula; MB, mushroom body; ME, medulla; ml, mid-line of brain; MNC, medial neurosecretory cells; NCC, nervus corpus cardiacum; OL, optic lobe; PDF, pigment dispersing factor; PTTH, prothoracicotropic hormone; rCAp, cell body rind posterior to the calyx of the MB; rLAl, optic lobe cell body rind lateral to LA surface; rMEd, optic lobe cell body rind dorsal to ME rind; rMEp, optic lobe cell body rind posterior to ME rind; rSLPl, superior cell body rind lateral to SLP; rSLPp, superior cell body rind posterior to SLP; rSMPa, superior cell body rind anterior to SMP; rSMPmp, cell body rind along the midline medioposterior to SMP; 5HT, serotonin; SIP, superior intermediate protocerebrum; SLP, superior lateral protocerebrum; SMP, superior medial protocerebrum; SP, superior protocerebrum

* Corresponding author at: Biology Department, York University, 4700 Keele Street, Toronto, Ontario M3J 1P3, Canada.
E-mail addresses: xanthev@yorku.ca (X. Vafopoulou), csteel@yorku.ca (C.G.H. Steel).

https://doi.org/10.1016/j.ygcen.2018.07.012
Received 1 May 2018; Received in revised form 16 July 2018; Accepted 20 July 2018
Available online 23 July 2018

studied (e.g. review by Crane and Young, 2014), as has the neural organization of the circadian system in the brain (reviews by Helfrich-Förster, 2014; Meelkop et al., 2011; Taghert and Nitabach, 2012; Vansteensel et al., 2008) and several of the output rhythms, including both behavioral rhythms (e.g. reviews by Helfrich-Förster, 2014, 2018; Meelkop et al., 2011; Nässel and Winther, 2010; Numata et al., 2015) and endocrine rhythms (reviews by Bloch et al., 2013; Numata et al., 2015; Tomioka, 2014; Vafopoulou and Steel, 2009, 2012; Uryu et al., 2015).

This laboratory has analyzed the properties and regulation of circadian rhythms of various key insect hormones in *R. prolixus*, including several neurohormones essential for growth and development, such as PTTH (Vafopoulou and Steel, 1996a,b, 2002; Vafopoulou et al., 2007), testis ecdysiotropin (Vafopoulou and Steel, 2005) and insulin-like peptide (Vafopoulou and Steel, 2012a). We have analyzed their roles as 'messengers of time' to target issues in *R. prolixus*, and found that the primary regulatory circadian system is located in the brain, as it is in most animals. The neuroanatomical organization of this clock system has been described in detail for *R. prolixus* (Vafopoulou et al., 2010; Vafopoulou and Steel, 2012b). The principle group of circadian clock cells, the lateral cells (LNs) are located in the proximal OL and slightly dorsal to AME, which is a small ovoid appendix to the ME in the OL. LNs express the canonical clock proteins PERIOD and TIMELESS and are readily identified by the abundance of pigment dispersing factor (PDF) IR throughout both cell bodies and neurites (Vafopoulou et al., 2010; Vafopoulou and Steel, 2012b). In many species, the AME and its associated cells have been shown by various techniques to be a central component of the circadian clock system (e.g. Page, 1982; Sokolove, 1975; reviews by Helfrich-Förster, 2014; Homberg et al., 2003; Stengl and Arendt, 2016; Wei et al., 2010). In *R. prolixus*, the LN axons project ventrally into the AME, where they ramify extensively, a phenomenon observed in all other insects examined. Then, the LN axons project distally to the OL and proximally to the protocerebrum, primarily to the dorsal surface of SLP and to a lesser extent, on the dorsal surface of SIP and SMP (Vafopoulou et al., 2010; Vafopoulou and Steel, 2012b) (summarized in Fig. 1). We have named this area of dense arborizations the area of principle protocerebral arborizations (PPA) of the LNs (Vafopoulou et al., 2010). In other insects, the neurites of comparable PDF-IR clock cells in the AME area may take routes to the OL and the SP that differ slightly from that of *R. prolixus,* but all conform to a similar general pattern. An overview of the main pathways of the LNs in the circadian system in the brain of *R. prolixus* larva is presented in Fig. 1 (for details see Vafopoulou et al., 2010).

The AME of many species also contains a variety of axons other than those of the LNs, (e.g. Homberg et al., 2003; Petri et al., 1995; Stengl and Arendt, 2016). There is an abundance of other cells in the AME and ultrastructural studies of them showed both afferent and efferent synapses on PDF axons (e.g. Reischig and Stengl, 2003; Wei et al., 2010), suggesting extensive input and/or output of information from the circadian system in this neuropil. Collectively, this information has led to the view that the AME represents a major synaptic integration center in the circadian system (reviews by Helfrich-Förster, 2009; Homberg et al., 2003; Stengl and Arendt, 2016) and it has been compared with the mammalian suprachiasmatic nucleus (Helfrich-Förster, 2004).

In the SP of *R. prolixus*, there are numerous probable close associations between LN neurites in the PPA and neurohormone-producing cells such as PTTH (Vafopoulou et al., 2007), insulin-like neurohormone (Vafopoulou and Steel, 2012a) and testis ecdysiotropin (Vafopoulou and Steel, 2005). Less conspicuous arborizations of LNs have been reported in this area in other species (review by Homberg et al., 2003), but this area has received little experimental attention until very recently. Recent studies in *Drosophila* showed that PDF conveyed circadian information from clock cells to cells in SP, such as PTTH-producing cells (Selcho et al., 2017), AstA producing cells (Chen et al., 2016) and several pars intercerebralis cells (Cavanaugh et al., 2014).

A key area of ignorance that remains in *R. prolixus* is the neural pathways by which the brain circadian clock communicates the timing information that regulates the rhythmic release of these hormones. The present paper studies several neuron types, which emerge as associated with the circadian system in *R. prolixus*, identifies possible centers of integration in the circadian system in the brain and evaluates the importance of AME and PPA as centers for integration. We examined the pathways in the SP and the OL of cells that are IR to three neuropeptides, AstA-7, CCAP, FMRFamide, and 5HT. These four molecules were selected because they have been shown to be components of the circadian network in several insects (e.g. Homberg et al., 2003; Meinertzhagen and Pyza, 1999; Petri et al., 1995; Würden and Ito et al. (2014).

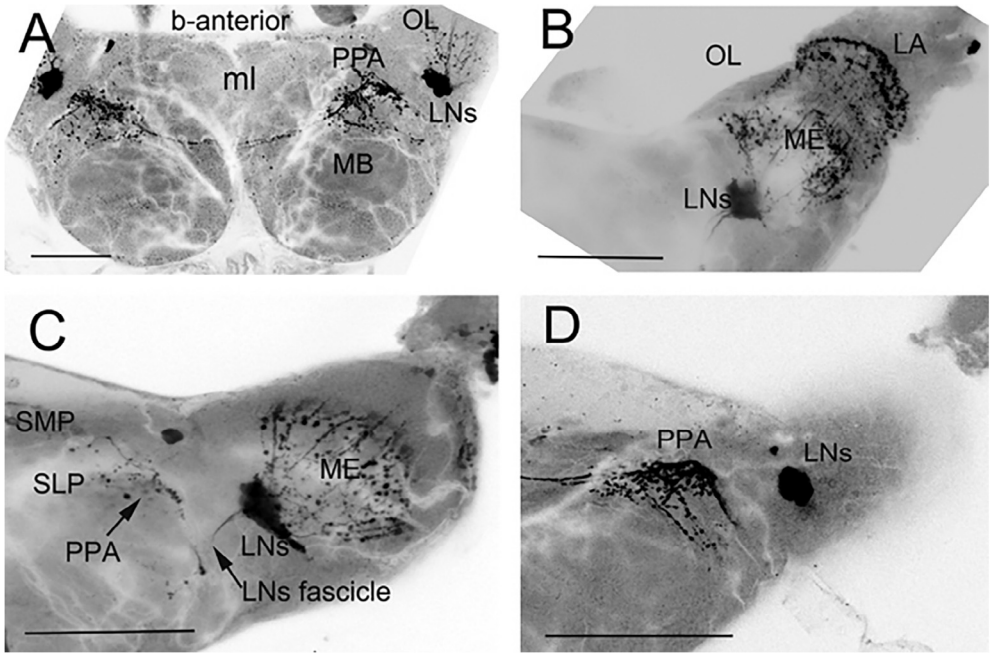

Fig. 1. Overview of LNs and their projections in the dorsal side of the SP as revealed by PDF-IR. The gray scale is inverted to depict intense fluorescence as black. A is a stack of 35 sections; B-D are stacks of 10 sections each from the same series; B is the most ventral and D the most dorsal stack. A. The general plan of the ramifications of the LNs in a whole brain. LNs are located at the border of the SP with the OL and belong to the OL cell body rind dorsal to ME rim. LN axons project to the superior neuropils where they arborize extensively to form a densely arborized area, which we term the principle protocerebral arborization area (PPA), located anterior to the MB. Some axons from PPA cross the ml to the contralateral PPA. B. OL showing LN projections distal to the ME, the AME and the LA. C. LNs also project proximally to the SLP and the SMP; arrow shows a sharp deep loop that LN axons take, before they emerge on the surface of SLP. D. The proximal LN projections arborize primarily on the dorsal surface of the SLP and to a lesser extent in the SMP. Scale bars = 50 μm. Nomenclature for brain regions throughout is according to

Homberg, 1995; see also Discussion). They also have important pleiotropic roles in diverse physiological and behavioral functions in insects, including *R. prolixus* (e.g. for AstA, review by Nässel, 2002; for CCAP, reviews by Gäde and Hoffmann ,2005; Mykles et al., 2010; Nässel, 2002; for FMRFamide reviews by Krajniak, 2013; Mykles et al., 2010; Nässel, 2002; for 5HT reviews by Blenau and Thamm, 2011; Ellen and Mercer, 2012; Orchard, 2006). These four molecules are members of the spectrum of mediators of neurochemical communication among cells and tissues, functioning variously as neurotransmitters, neuromodulators or neurohormones to various degrees in different physiological systems. In the present work, we found a complex and intricate network of IR cells and neurites in the brain of *R. prolixus*. The neurites of all these IR cells possess varicosities within the brain; varicosities are classically regarded as sites of release of neuromodulators. In addition, IR neurite types projected to known neurohemal organs where their contents can be released as neurohormones. Indeed, in *R. prolixus*, these molecules have either been detected in the hemolymph (for 5HT Orchard, 2006; for FMRFamide-like peptides, Elia et al., 1993; Tsang and Orchard, 1991) or are likely to be released into the hemolymph (for AstA, Sarkar et al., 2003; for CCAP, Lee and Lange, 2011; Lee et al., 2011). While we expect that classical synapses also occur among these IR axons within the brain, their detection is beyond the resolution of the confocal microscopy used here. Our observations suggest that these four molecules appear to act mainly as neuromodulators and/or neurohormones in the *R. prolixus* brain. In addition, we report that few neurites of these four cell types enter the AME, but rather project directly to the ME and/or LA neuropils or the PPA. It appears that in *R. prolixus* the PPA is an area of equal importance to the AME of other species. These findings indicate that the ME, LA and PPA are major integration areas of circadian information, whereas the role of the AME appears relatively modest in *R. prolixus*.

2. Materials and Methods

2.1. Animals

Fifth (last) larval instars of *R. prolixus* were raised in a 12 h light: 12 h dark cycle at 28 °C ± 0.5 °C. Unfed larvae exist in a state of arrested development resembling diapause, but remain behaviorally active. Development to the adult stage is initiated by a blood meal and ecdysis to the adult occurs at about 21 days after feeding. Only male fifth instar animals were used at day 12 after feeding; brains were excised in mid-scotophase at 7 h after lights-off, as it is known that at this time PDF staining of LNs in the brain is intense (Vafopoulou et al., 2010).

2.2. Antibodies

A mouse monoclonal antibody raised against a synthetic AstA-7 (APSGAQRKYGFGL-NH_2; Woodhead et al., 1989) from *Diploptera punctata* was purchased from Developmental Studies Hybridoma Bank (5F10 supernatant; University of Iowa, IA) and was used at a dilution 1:1000. AstA-7, a tridecapeptide, is a member of the AstA subfamily. Allatostatins are a large group of neuropeptides and are divided into three families, the A-, B-, and C-types. AstA peptides were first identified from the cockroach *D. punctata* (Woodhead et al., 1989) and have a conserved pentapeptide C-terminal sequence (F/YXFGLamide), which is the minimum structural requirement for biological activity. The present antibody shows very low cross-reactivity with other Ast peptides (Stay et al., 1992). This antibody has been used to identify AstA-containing cells immunohistochemically in several insects, including *Diploptera* and *Drosophila melanogaster* (Stay et al., 1992; Yoon and Stay, 1995). In *R. prolixus*, the *Diploptera* AstA-7 exhibits biological activity by inducing inhibition of hindgut contractions *in vitro* (Sarkar et al., 2003). The peptide was also localized in midgut endocrine cells (Sarkar et al., 2003) and is considered a brain/gut peptide. Genomic, biochemical and physiological evidence showed that *R. prolixus* possesses AstA-like peptides; neuropeptidome analysis identified Ast sequences in the *R. prolixus* genome (Ons et al., 2009) and more recently the entire cDNA sequence of *R. prolixus* AstA has been cloned (Zandawala et al., 2012) and a functional receptor for AstA has been identified and characterized (Zandawala and Orchard, 2015). Here, preadsorption of the antibody with excess (100 μM) synthetic AstA-7 (Sigma, St. Louis, Mo., USA) abolished all IR. We have not shown that IR to this antibody is specific for AstA-7, and therefore we term IR to the *Diploptera* antibody as AstA-IR.

A rabbit polyclonal antiserum produced against a synthetic peptide corresponding to N-terminal residues of *D. melanogaster* CCAP and conjugated to glutaraldehyde/polylysine was purchased from JenaBioscience (Jena, Germany) and was used at a dilution of 1:800. This anti-CCAP was tested by the manufacturer for cross-reactivity with other similar peptides by ELISA. CCAP is a cyclic amidated nonapeptide first isolated from the pericardial organs of the shore crab *Carcinus maenas* (PFCNAFTGCamide; Stangier et al., 1987) and is highly conserved among arthropods. The amino acid sequence of *R. prolixus* CCAP is identical to that of *C. maenas* (Lee and Lange, 2011) and a functional receptor has been identified (Lee et al., 2013). CCAP in *R. prolixus* exhibits myotropic activity on the hindgut (Lee and Lange, 2011) and oviduct (Donini and Lange, 2002) and modulates heart rate and beat (Lee and Lange, 2011). In *R. prolixus*, the specificity of the antibody was verified by pre-adsorption with excess CCAP (1 mg/ml; MyBioSource, San Diego, CA), which completely abolished fluorescence in the brain. IR to anti-CCAP is called here CCAP-IR.

A rat polyclonal antiserum against synthetic 5HT conjugated to bovine serum albumin was purchased from MediCorp (1019-003 supernatant; Montreal, QC) and was used at a dilution of 1:500. The specificity of 5HT-IR was verified by pre-adsorption of the antibody with excess 5HT (1 mg/mL; Sigma-Aldrich; St. Louis, MO), which completely abolished fluorescence in the brain. 5-HT-IR is widespread in the *R. prolixus* central and peripheral nervous system (Lange et al., 1988). In *R. prolixus*, 5-HT plays a central role in the behavior and physiology of feeding; it acts as a diuretic hormone, affects salivary gland secretion, cuticular plasticization, cardioacceleration and modulates muscle contractions (review by Orchard, 2006). A functional receptor type-2B has also been identified (Paluzzi et al., 2015).

A rabbit polyclonal antiserum against FMRFamide was purchased from ImmunoStar (Hudson, WI) and was used at a dilution of 1:500. It was raised against synthetic FMRFamide conjugated to bovine thyroglobulin. FMRFamide is a tetrapeptide member of a large superfamily of FMRFamide-like peptides (FLPs) with several subfamilies (review by Audsley and Weaver, 2009; Krajniak, 2013). In *R. prolixus*, FLPs are distributed throughout the central nervous system and peripheral organs (Sedra and Lange, 2014; Tsang and Orchard, 1991). They modulate the frequency of heart contractions and the contractions of midgut and hindgut (Lee et al., 2012) and oviduct (Sedra and Lange, 2014; Sedra et al., 2015) and egg production (Sedra and Lange, 2016). Neuropeptidome analysis of the *R. prolixus* genome (Ons et al., 2009) and the above immunohistochemical studies have shown that *R. prolixus* possesses FLPs. A subfamily of the FLPs includes the myosuppressins. A myosuppressin was isolated from *R. prolixus* with a unique FMRFamide C-terminal (Lee et al., 2012). In the present study, the specificity of the antibody was examined by pre-adsorption of the antibody with excess FMRFamide (1 mg/mL; Sigma-Aldrich) and only very faint IR remained in the brain. However, antisera developed against FMRFamide most likely recognize the epitope formed by the C-terminal RFamide and hence will cross-react with a broad spectrum of FLPs (see Nässel, 2002). We cannot exclude cross-reactivity with other FLPs, such as the above mentioned *R. prolixus* myosuppressin (Lee et al., 2012), so IR to this antibody is called FLP-IR.

A guinea pig polyclonal antiserum against a custom-made, synthetic peptide of the complete amino acid sequence of *Uca pugilator* pigment dispersing hormone, known as PDF in insects, (NSELINSILGLPKVMDA)

(GenScript, Piscataway, NJ) and was used at a dilution of 1:500. All PDFs known have a homologous structure to pigment dispersing hormone (e.g. Singaravel et al., 2003). PDF is considered to be an output of the LNs, has diverse functions in the circadian system (reviewed by Helfrich-Förster, 2009; Nässel and Winther, 2010; Taghert and Nitabach, 2012) and has been used extensively to trace LN axonal projections in many insects (e.g. reviews by Helfrich-Förster, 2014; Homberg, et al., 2003). We have used the present antibody before to trace the projections of LN neurites in *R. prolixus* brain (Vafopoulou and Steel, 2014).

Goat anti-rabbit IgG conjugated to the green fluorophore FITC was used as secondary antibody with anti-CCAP and anti-FMRF-amide. Goat anti-mouse and anti-rat IgGs conjugated to FITC were used as secondary antibodies to anti-AstA-7 and anti-5HT respectively. Goat anti-guinea pig IgG conjugated to the red fluorophore TRITC was used as the secondary antibody with anti-PDF. All secondary antibodies were purchased from Sigma-Aldrich and were used at 1:200 dilutions.

2.3. Fluorescence immunohistochemistry and imaging

The procedure for preparations of whole mounts of brains treated with primary and secondary antibodies has been described before in detail (Vafopoulou et al., 2010). In controls, the primary antibodies were replaced with non-immune serum or were subjected to preadsorption (see above), or the secondary antibodies were replaced with PBS. Fluorescence levels in controls were indistinguishable from the background and autofluorescence was not detected. Digital optical sections were viewed using an Olympus FV300 confocal laser scanning microscope at intervals of 1 µm. When both red and green fluorescent neurites are seen in extremely close proximity, or in many cases overlapping each other, this creates a small region of yellow fluorescence in a 1 µm optical section, implying that the two differently fluorescent neurite types are probably within 1 µm of each other at that point, suggesting that communication between them may occur at these loci. We describe these regions of close associations as loci of close or tight superimposition or superposition throughout the text. Parameters of the microscope were kept constant for all image capture. Images were processed using Image J (1.50 h; NIH, Bethesda, MD) and Adobe Photoshop CS5 (San Jose, CA). Visual enhancement was achieved in several images by inversion of the gray scale (Figs. 1, 2, 4, 6, 8) so that intense fluorescence appears black on a light background. Figures show the dorsal aspect of the right brain hemisphere, with the exception of panoramic views, which show both hemispheres. All neuronal IR was cytoplasmic. Both somata and neurites were IR, enabling us to trace the pathways of specific neuron types for long distances.

3. Results

3.1. AstA-IR cells

Several regions in the SP (Fig. 2A) contain AstA-IR cells and neurites. In the OL, a dense web of AstA-IR neurites is seen in the ME (Fig. 2B). These emerge from the distal side and were traced distally through the LA (Fig. 2F, G) into the optic tract and into the compound eye, where they terminated in large numbers of very elongated cell bodies (Fig. 2C–E). These cell bodies were located just below the cornea and their axes were all roughly parallel, suggesting they are components of the ommatidia. Higher magnification images were not possible for technical reasons. However, careful examination of images such as Fig. 2C (arrow) reveals that the AstA-IR neurites are surrounded by a ring of six larger cells each of which contains a darker spot that seems to represent pigment. There is only one AstA-IR cell per ommatidium. In *R. prolixus*, a ring of six retinula cells 1–6 (R1–6) surrounds a central pair of retinula cells 7 and 8 (R7–8). It is one of this central pair (R7/8) that is AST-IR. Each has a long axon that projects through the LA (Fig. 2F) and terminates in the ME (Fig. 2G). No other cells in the OL were revealed with anti-AstA.

Three anatomically separate groups of AstA-IR cells were seen in the PR (Fig. 2A). First, 2–3 rSMPa strongly fluorescent cells occur about 60 µm below the dorsal surface, projecting towards the SMP (Fig. 2A). Second, at the border of the optic lobe with the SLP, a group of about 10 rSLPl and rSLPp cells was located (average size about 8–10 µm in diameter) (Fig. 2A, B); these cells projected neurites medially towards the SLP and possibly beyond (Fig. 2H, I). Slightly dorsal to the rSLPp cells, but within this group, a large and strongly IR neuron was seen, called here Maximus (Max-rSLPp cell) (about 25 µm in diameter) (Fig. 2A, white arrow; 2I, J). A cluster of 4–5 small cells was juxtaposed to Max-rSLPp cell. This cluster and Max-rSLPp both projected neurites as a fascicle postero-medially along the anterior border of the MB (Fig. 2A). This fascicle bifurcated on the antero-medial side of the MB (Fig. 2A, long black arrow; Fig. 2J); one branch followed an antero-medial trajectory and arborized extensively in the dorsal surface of the SMP. The second branch of the fascicle projected posteriorly, exited the SP via the NCC (Fig. 2A, black arrow; Fig. 2K) and terminated on the dorsal vessel (not shown). The large size of this cell and its projection to the dorsal vessel suggest that it may be a neurosecretory neuron. The third group of AstA-IR cells are rSMPmp cells and project neurites anteriorly, which arborize in the dorsal surface of the SMP (Fig. 2K, L, arrows).

Thus, the arborizations of all the above three groups of AST-7-IR cells occur in the dorsal region of the SP, forming an immense web of neurites with many varicosities in the broader area where PPA is located (Fig. 2A; see also Fig. 3E). This area was also enriched by axonal projections from several other AstA-IR cells scattered in this area (Fig. 2M, arrows) that extended over most of the dorsolateral surface of the SP all the way to the ml. Many neurites crossed the ml, but their trajectories were difficult to follow (Fig. 2M). It is possible that these neurites also arborize in the contralateral brain hemisphere, potentially providing a further means of coupling of left and right brain hemispheres.

3.2. Association of AstA-IR cells with clock cells

The associations of AstA-IR cells with LNs were elucidated using antisera to anti-AstA-7 (left column; green channel) and anti-PDF (third column from left; red channel). In the panoramic dorsal view of the brain (Fig. 3A–C), the distal optic lobes are out of focus and not included. Tight superimposition of AstA-IR and PDF-IR (yellow/orange) occurs in the lateral aspect of the SP. Enlarged views of specific areas (indicated below) are shown in the ‘enlarged’ column at the far right of Fig. 3. Fig. 3D–F shows an enlarged dorsal view of the right brain hemisphere that includes the optic lobe. Two areas of interest were examined in detail; box ‘a’ in Fig. 3E includes the LNs, box ‘b’ includes the PPA.

Images in Fig. 3G-I1, Fig. 3J-L1 and Fig. 3M-O1 were taken from the same series, J-L1 being more ventral than G-I1; Fig. 3M-O1 is from the same plane of focus as Fig. 3J-L1. Some of the terminations of the retinula cell neurites in the ME occur in varicosities that are closely apposed to varicosities of the LNs in the ME (Fig. 3H); the box in Fig. 3H is shown enlarged in Fig. 3I1. Although the varicosities of both neuron types are in close proximity in this area, there are no regions of yellow indicative of superimposition of the two neurite types. However, if AstA and/or PDF function as neuromodulators in this area, they could readily influence one another. A similar arrangement occurs more ventrally (Fig. 3K); here, retinula cell terminations in the ME are seen in very close proximity to the AME. But the enlarged image of the box in Fig. 3K, shown in Fig. 3L1, again shows proximity of the two axon types but not superimposition. The retinula cell neurites do not appear to penetrate the AME.

In contrast to the above observations, there is clear evidence of close superposition between the retinula cell neurites and LN neurites more laterally, in the LA (Fig. 3M-O1). The box outlined in Fig. 3N is enlarged in Fig. 3O1, in which yellow superpositions between the two axon types

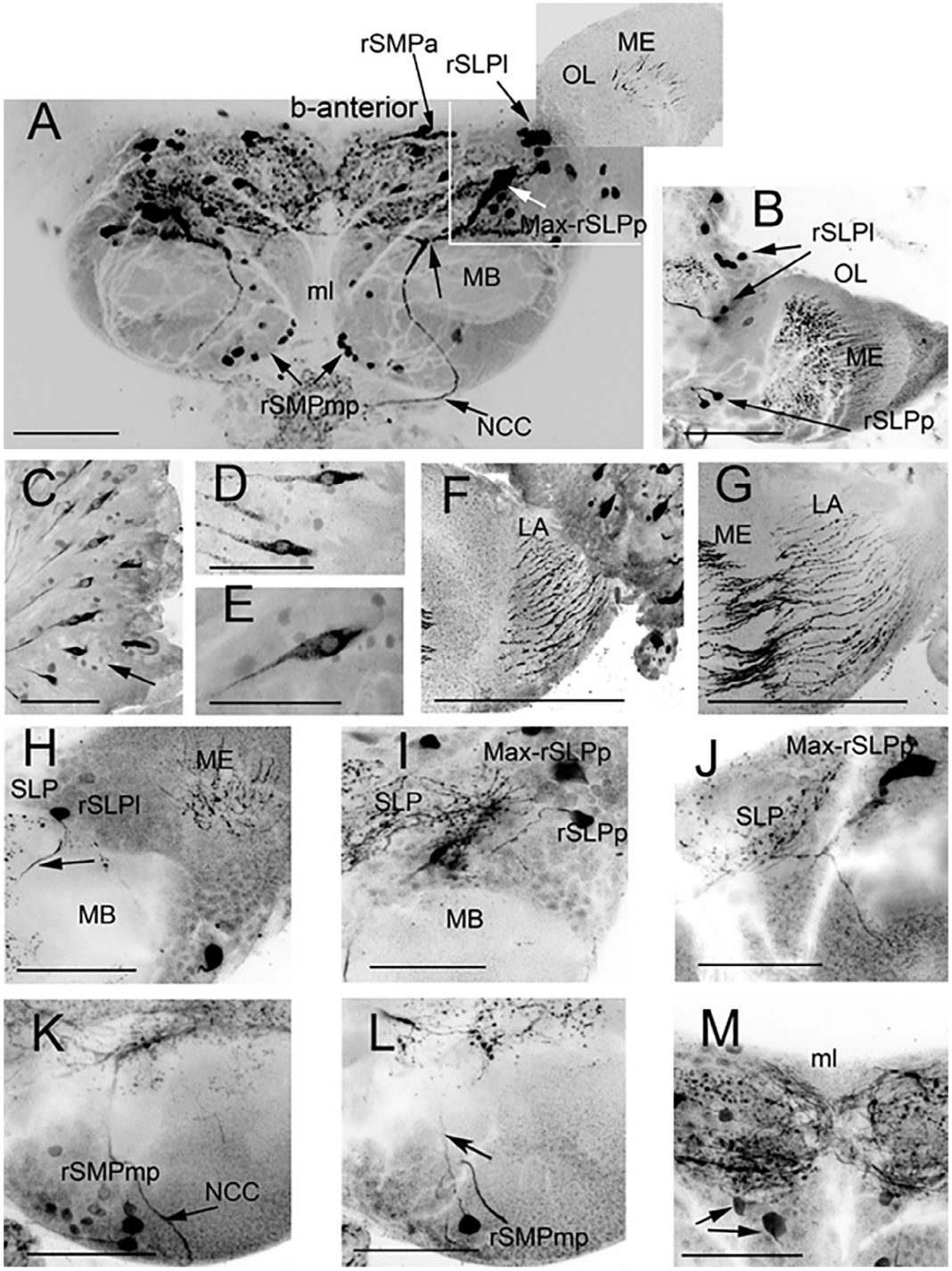

Fig. 2. AstA-IR neurons in the dorsal brain and OL. The gray scale is inverted to depict intense fluorescence as black. A and B are stacks of 26 sections each. C-F are 1 μm sections. G is a stack of 60 sections. H-M are stacks of 5 sections each. A. The general plan of the ramifications of the AstA-IR cells in the brain and OL; AstA-IR neurites are seen in the ME and in a broad region anterior to MB in the SMP and SLP. Cell bodies giving rise to these neurites are termed rSLPp (including Maximus, abbreviated as Max-rSLPp), rSLPl, and rSMPa and rSMPmp. B. AstA-IR neurites in ME and neurites from rSLPl. C. Ommatidia with retinula cells 1–6 (R1-6) arranged in a ring surrounding a single AstA-IR retinula cell (R7/8; arrow) and its axon. D-E. Higher magnifications of R7/8. F. A section dorsal to D and E, showing R7/8 axons travel to the LA. G. A large number of IR axons in parallel formation from R7/8 project through the LA to ME. H. AstA-IR axons in the ME and a rSLPl cell projecting an axon (arrow) to SLP. I-J. Are from the same series, I being ventral to J: I. The position of Max-rSLPp and another rSLPp neuron. J. Max-rSLPp. K-L. Are taken from the same series, J being ventral to K: K. The axon of Max-rSLPp about to enter the NCC (arrow) and many rSMPmp cells. L. rSMPmp cell projecting an axon anteriorly (arrow) toward the SMP, not towards the NCC. M. AstA-IR neurites crossing the ml. Arrows shows ASTA-IR cells scattered on the surface of the SP. Scale bars = 50 μm in A and B; 20 μm in C-F; 30 μm in G-M.

are obvious (arrows). In this area, it is possible that essentially unprocessed visual information could be communicated from the eye directly to the LNs, or that the LNs could transfer circadian information to the retinula cells (see Section 4.1). In the SP, visual contacts between PDF-IR neurites from the LNs and AstA-IR neurites were seen only in the SLP. Several contacts of LN neurites appeared to occur in the vicinity of Max-rSLPp cell and its companion small cells; this area is outlined by the box in Fig. 3E. Enlargements of this box are shown in

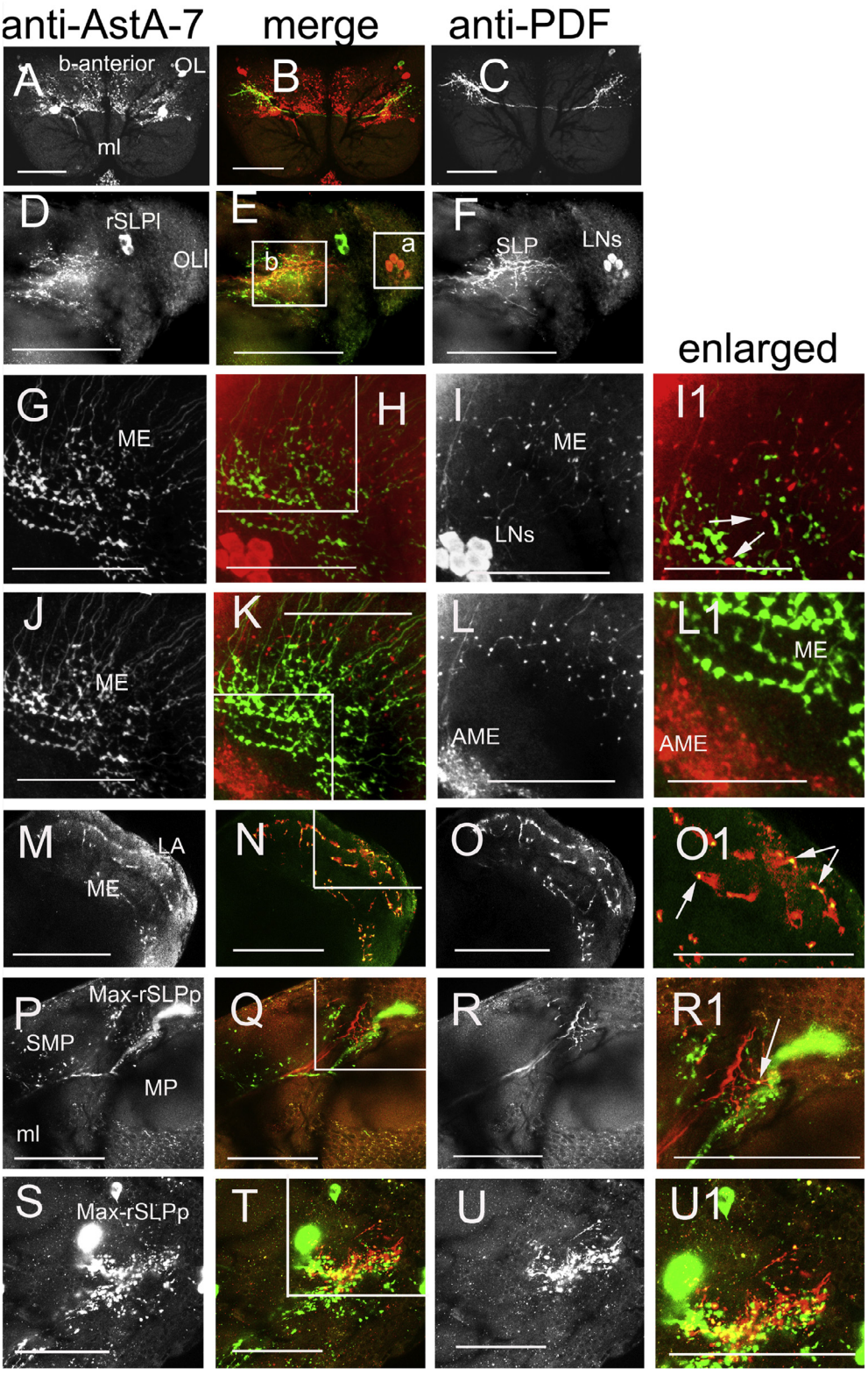

Fig. 3. AstA-IR (left column, green) related to PDF IR neurites from LNs (right column, red). Merged images of left and right are shown in the merge column. Tight superimposition of the two types shows as orange/yellow. All images are dorsal views of the brain and OL. A-F are images of 17 sections each. G-R1 are 1 µm sections. A-C. Panoramic view of a brain showing the ASTA-IR and PDF-IR neurites in the brain. D-F. Enlarged images of the right brain hemisphere and OL show AstA-IR rSLPl cells and the LNs and their arborizations in SLP in the merged image E. Detailed associations of AstA neurites and LN neurites in OL is shown in enlarged areas of box "a" (G-O1) and for the rSLPl neurons in SP in box "b" (P-X1). G-O1 are from the same series; G-I1 is dorsal to J-L1, which is is on the same plane of focus as M-O1. G-I1. ME and LNs; several AstA-IR retinula cell varicosities are adjacent to PDF-IR varicosities as shown in the enlarged image in I1 (arrows) of the box in H. J-L1. ME and AME. The AstA-IR neurites in ME appear to terminate near AME in L1, which is the enlarged image of the box in K. M-O1. Tight superimposition is seen in LA of AstA-IR retinula cell neurites and PDF-IR neurites in O1 (arrows), which is enlargement of the box shown in N. P-U1 are all from the same series, P-R1 being the most dorsal and S-U1 being the most ventral. P-R1. Axon of Max-rSLPl cell runs parallel to PDF-IR axons; the two types of neurites are rarely seen superimposed in RI, which is enlargement of the box in Q. S-U1. Ventral to P-R1, the paths of the two types of neurites are tightly superimposed as seen in U1, which is enlargement of the box in T. The two neurite types arborize widely; abundant tight superimpositions of AstA-IR varicosities and PDF-IR varicosities are seen. Scale bars = 50 µm in A-F; 30 µm in G-U11; 20 µm in enlarged images I1, L1, O1, R1, U1.

Fig. 3P-R1 and Fig. 3S-U1. Both images are from the same series, but Fig. 3P-R1 is dorsal to Fig. 3 S-U1. In the more dorsal image, points of close superposition are seen, but are not abundant (arrow in Fig. 3R1). Further ventrally, abundant arborizations of Maximus appear and numerous close superpositions occur with the neurites of the LNs (Fig. 3U1, arrows). Therefore, there is extensive potential for exchange of information between these AstA-IR rSLPp cells and LNs in the SLP. The jungle of neurites in this area precluded determination of exactly which AstA-IR cells were involved. In conclusion, there is potentially direct communication between the AstA-IR cells and LNs in the SLP. In the case of the Max-rSLPp neuron, its potentially neurosecretory nature raises the possibility of clock control of hormone release from this cell from the dorsal vessel, and possibly of other AstA-IR cells in the PPA.

3.3. CCAP-IR cells

Five groups of CCAP-IR cell somata were identified in each brain hemisphere, two groups in the OL, and three groups in the SP (Fig. 4A, B).

In the distal tip of the OL, numerous, possibly hundreds, of superficial CCAP-IR rLAl cell bodies were seen, arranged mostly in a monolayer. They projected CCAP-IR neurites (Fig. 4B, D, E) primarily to the LA (Fig. 4D), and possibly also to the ME, which is richly innervated with CCAP-IR neurites (Fig. 3C). The majority of these cells were small (about 3–4 μm in diameter) (Fig. 4B, D) with a few larger size cells (about 5–6 μm in diameter) among them (Fig. 4E).

In the proximal region of the optic lobe at the border with the SLP, approximately 10–15 rMEd cells (about 10 μm in diameter) are seen. All detected rMEd cells project to the ME and not to the AME. One such cell is shown in Fig. 4F projecting its neurite ventro-laterally to the ME. This is shown more clearly in brains labelled with both anti-CCAP and anti-PDF in Fig. 5J–L (described in Section 3.4). These projections were difficult to follow within the ME, but they may reach the LA and contribute to the abundant CCAP-IR there. Thus, the rLAl cells seem positioned to make intimate contacts with rMEd in both the ME and LA.

Only a few CCAP-IR fibers were seen in the AME (Fig. 4G, arrow).

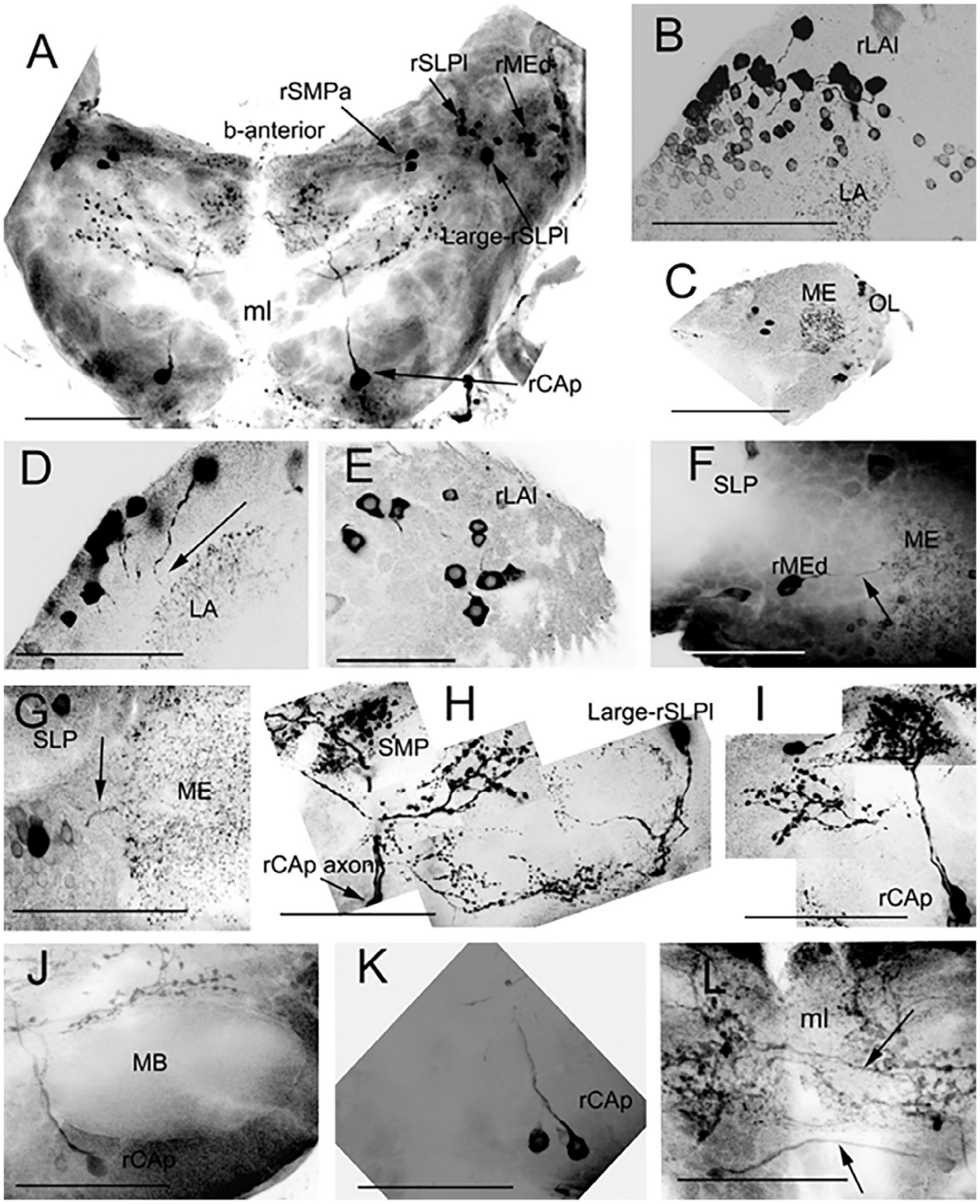

Fig. 4. CCAP-IR neurons and their projections. The gray scale is inverted to depict intense fluorescence as black. All images are dorsal views of the optic lobe and brain. A-C, H and I are stacks of 25 sections each. D, F, G, J-L are stacks of 5 sections each. E is 1 μm section. A. The general plan of IR neuron locations: rMEd cells in OL; rSLPl cells and the Large-rSLPl cell which project axons to SLP and SMP; rCAp cells which project axons to SMP. B, D. Numerous rLAl cells, project axons to LA (arrow in D). C. shows neurites in ME. F. A rMEd cell projecting its axon to ME (arrow). G. A rare example of a neurite traversing the AME (arrow). H. Pathway of the axon of the Large-rSLPl toward the SMP where it arborizes extensively. I-K. The fascicle of the two rCAp cells project anteriorly (J, K) toward the SMP and arborize in it (I). L. Numerous neurites (arrows) cross the ml. Scale bars = 50 μm.

Details of these fine projections in the AME are shown in preparations using both anti-CCAP and anti-PDF in Fig. 5D–I. The origin and destination of these fine fibers is unknown. It is also unclear whether they terminate in the AME or pass through it. Occasional CCAP-IR neurites (presumably from rMEd cells) emerge from the ME and seem to pass through the AME (Fig. 4G, arrow). It is concluded that CCAP-IR cells located both distally (rLAl cells) and proximally (rMEd cells) in the OL project their neurites primarily into the ME and LA where they arborize, but seldom project to, or arborize in, the AME.

Three groups of CCAP-IR cells were seen in the SP, each consisting of only a small number of cells. The first group are about 10 rSLPl cells (about 10 µm in diameter, at a depth of about 40 µm from the surface) which projected neurites medially in the dorsal surface of the SLP (Fig. 4A). The Large rSLPl cell (about 20 µm in diameter), projected its

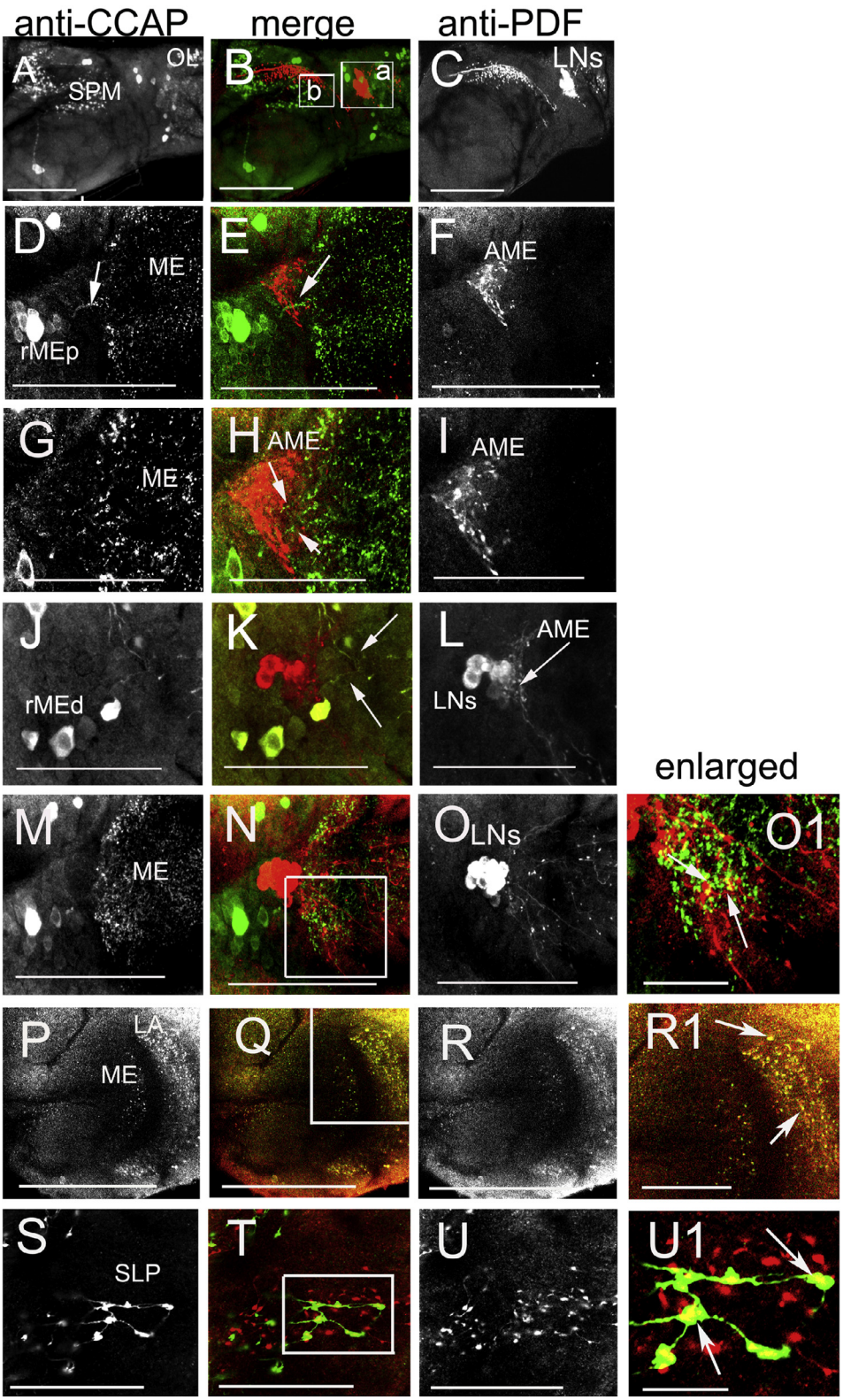

Fig. 5. Brains double labelled with anti-CCAP (left column, green) and anti- PDF (right column, red). Merged images of green and red are shown in the merge column. Tight superimpositions of neurite types are orange/yellow. All images are dorsal views of the optic lobe and the PR. A-C is a stack of 19 sections. D-U1 are 1 µm sections. A-C. Right brain hemisphere showing the LNs and the arborizations of their neurites with CCAP-IR neurites in the OL and PR. Associations between the two neuron types in the OL in box "a" are shown in D-R1, and associations in the SP in box "b" in S-U1. D-O1 are from the same series, D-F being ventral to M-O1. D-I. Few CCAP-IR fibers traverse the AME (arrows in E, H) in contrast to more abundant CCAP-IR in ME. J-LI. In a more dorsal plane of focus, rMEd cells project axons to ME that bypass the AME (arrows in K). M-O1. Numerous superimposed CCAP-IR varicosities with PDF-IR varicosities in ME in N; the box in N is shown enlarged in O1 (arrows). P-R1. Numerous tightly superimposed neurites of rLAl neurites and LN neurites in LA (see text), as shown in the enlarged image R1 (arrows) of the box in Q. S-U1. Tight superimposition between CCAP-IR varicosities and LN varicosities is also seen in SLP, as shown in the enlarged image U1 (arrows) of the box in T. Scale bars = 50 µm; in the enlarged images O1, R1 and U1, scale bars = 30 µm.

axon initially posteriorly and then medially along the anterior edge of the MB (Fig. 4H). This neurite then curved anteriorly to give rise to extensive arborizations in the dorsal region of the SMP. The second group comprised only two cells (about 10–12 μm in diameter), a doublet, located posterior to the calyx of the MB, the rCAp cells (Fig. 4A); these two cells project intertwined neurites anteriorly (Fig. 4J, K), and eventually arborize extensively in the dorsal region of the SMP (Fig. 4I, arrow). The third group are 2–4 rSMPa cells, which project neurites medially, but also to the SMP (Fig. 4A). Therefore, projections from all three groups of cells form an extensive area of CCAP-IR arborizations with numerous varicosities occupying a large area in the SP, mostly in the SMP (see Fig. 4A). It is possible that projections from the rMEd cells also arborize in the SP and contribute to this area as a pathway for exchange of information between the OL and the SP. CCAP-IR neurites (of unclear origin) also cross the ml (Fig. 4L), presumably providing further coupling pathways between the two sides of the brain.

3.4. Associations of CCAP-IR cells with clock cells

Brains were treated with both anti-CCAP (green channel) and anti-PDF (red channel) to reveal sites of potential associations between clock cells and CCAP-IR cells in the merge column (Fig. 5). Fig. 5A–C shows a dorsal panoramic view of the right brain hemisphere. In Fig. 5B, box 'a' includes the optic lobe and is enlarged in Fig. 5D-R1 and box 'b' includes the PPA and is enlarged in Fig. 5S-U1.

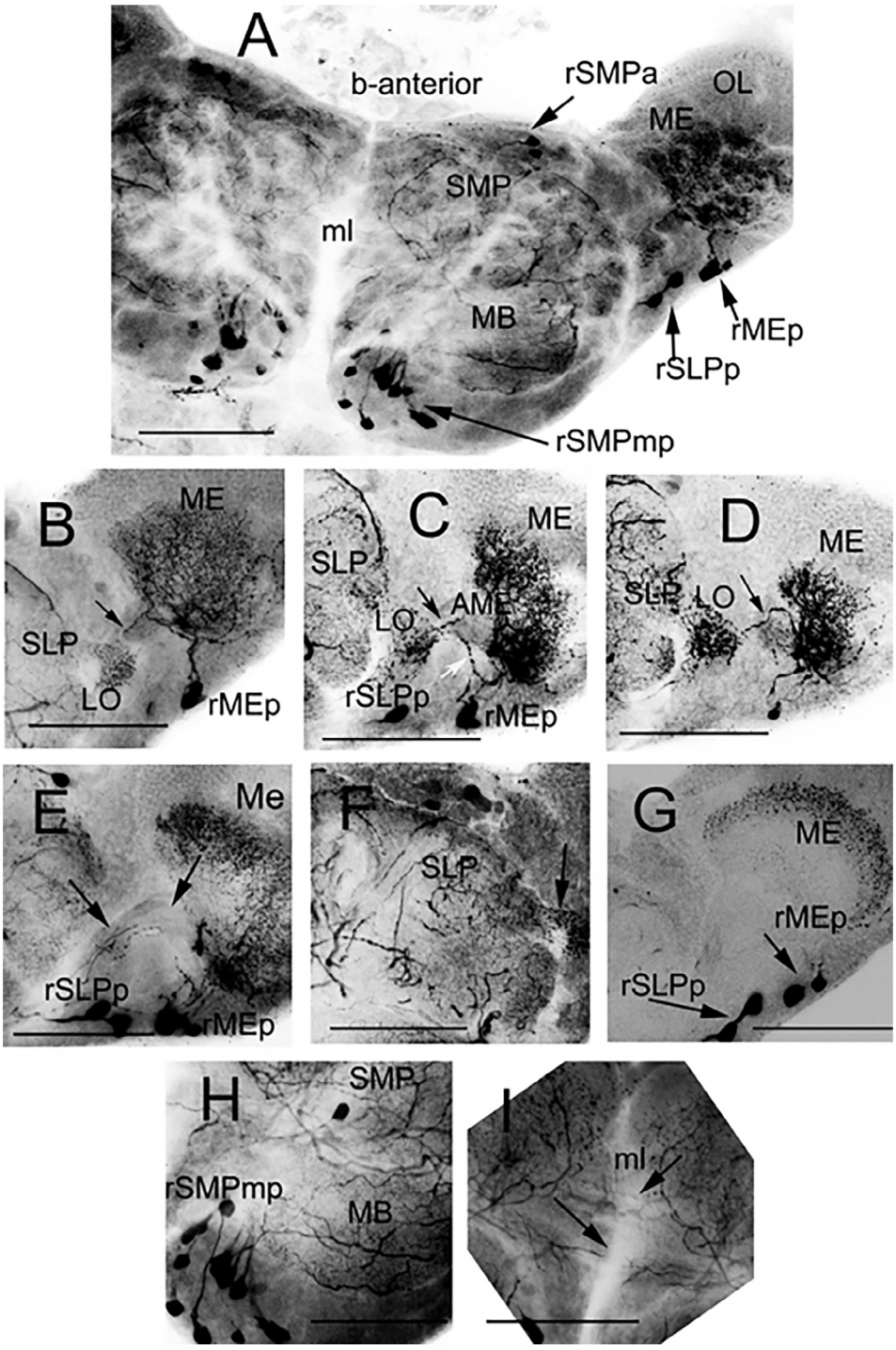

Fig. 6. 5HT-IR neurons and their projections. The gray scale is inverted to depict intense fluorescence as black. All images are dorsal views of the brain and OL. A is a stack of 30 sections. B-I are stacks of 10 sections each. A. Low magnification of the dorsal brain showing the general plan of the ramifications of 5HT-IR in the OL (rMEp cells) and in the SP (rSMPa cells, rSLPp cells and rSMPmp cells). B-E are from the same series, B being the most dorsal and E the most ventral. B. 5HT-IR rMEp project axons to strongly IR ME; arrow shows a neurite traversing the AME. C. This neurite (arrow) arborizes extensively in LO near a rSLPp cell. D. 5HT-IR fibers pass between LO and SLP; arrow shows a neurite crossing the AME. E. Numerous 5HT-IR neurites (arrows) emerging from ME projecting medially and posteriorly (arrows). F. A broad network of 5HT-IR neurites in the dorsal surface of SLP. G. 5HT-IR in rMEp and rSLPp cells. H. 5HT-IR rSMPmp cells project axons anteriorly towards SMP. I. 5HT-IR neurites cross ml (arrows). Scale bars = 50 μm.

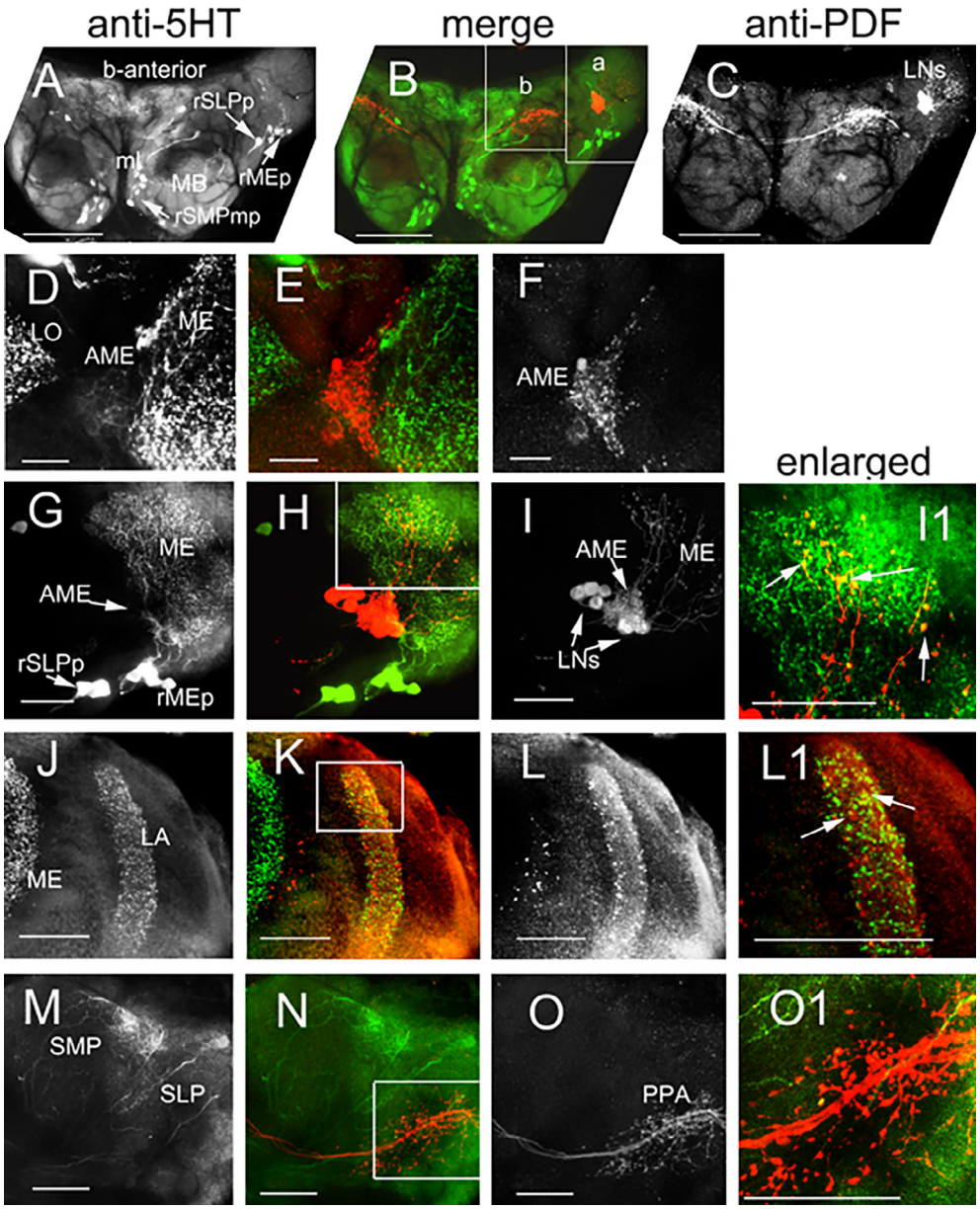

Fig. 7. 5HT-IR neurons and neurites (left column, green) in relation to PDF-IR LNs and neurites (right column, red). Merged images of left and right are shown in the merge column. Regions of tight superposition of the two types show as orange/yellow. All images are dorsal views of the PR and OL. A-C is a stack of 33 sections. D-O1 are 1 µm section each. A-C. Panoramic view of brain and OL showing 5HT-IR rMEp, sSLPp and rSMPmp cells in relation to the LNs. Associations between the two neuron types in the OL in box 'a' are shown in D-L1 and those for the SP in box 'b' are shown in M-O1. D-F. Many fine 5HT-IR neurites in AME in D but no tight superpositions with PDF-IR are seen in either AME or ME in the merged image E. G-I. Several 5-HT-IR rMEp cells appear to project primarily to ME but a few penetrate the AME; tight superimpositions are seen between 5HT-IR neurites and PDF-IR neurites in ME in I1 (white arrows), which is enlargement of the box in H. J-L1. LA shows proximities, but only rare areas of tight superimposition of the two neuron types (arrows in L1, which is enlarged from the box in K), although varicosities of the two neurite types are in close proximity. M-O1. No associations are seen in the SLP even though this is the primary neuropil of the PPA. Scale bars = 50 µm in A-C; 20 µm in D-O1.

Fig. 5D-O1 are from the same series, progressing from ventral (Fig. 5D–F) to dorsal (Fig. 5M-O1). Fig. 5D shows numerous CCAP-IR branches and varicosities in the ME, most likely from the rMEd cells (see Fig. 4F; Fig. 5S–U). In this plane of focus, Fig. 5F shows the AME, strongly fluorescent with PDF-IR neurites from the LNs. No superimposition between CCAP-IR and PDF-IR neurites was evident in either the ME or AME. In this plane, only one CCAP-IR fiber was seen traversing the AME (Fig. 5E, arrow); it passed through the AME, with no evidence of arborizations close to the LN neurites. More fine CCAP-IR fibers were visible in the AME in a more dorsal plane of focus (Fig. 5G–I; arrows in H). Even further dorsally, the LNs are seen, with their neurites fanning out in the ME (Fig. 5L), which is also strongly fluorescent with CCAP-IR neurites originating from the rMEd cells described above (Fig. 5J); still no superimpositions with PDF neurites were seen. By contrast, points of tight superimposition between CCAP-IR fibers and LN fibers were seen in the most dorsal section in Fig. 5M-O1 (arrows in Fig. 5O1). Thus, communication between LNs and CCAP-IR neurites is probable in the ME. Such communication also appears to occur in the LA (Fig. 5P-R1), where many points of superposition were seen in the enlarged region (Fig. 5R1) of Fig. 5Q. Therefore, in the OL, the LA and the ME are the main neuropils for potential communication between clock cells and CCAP-IR cells. If any such communication occurs in the AME, it appears to be very minor.

The SMP (the more distal part of the PPA) is the neuropil in which numerous CCAP-IR neurites are seen (Fig. 5S-U1) and where numerous points of superimposition occur (Fig. 5T) between the varicosities of CCAP-IR neurites (Fig. 5S) and PDF-IR neurites (Fig. 5U). Since several groups of CCAP-IR cells project to this area (Section 3.3), the cells of origin of these neurites could not be determined. As shown in Fig. 5U1, enlarged from the box in Fig. 5T, tight superposition of varicosities of CCAP neurites and LN neurites is seen in the SP, (primarily the SMP), indicating numerous points of potential communication between clock cells and CCAP-IR cells in the SP.

3.5. 5HT-IR cells

5HT-IR was detected in several discrete small groups of cells in the OL and in the dorsal side of the SP. A panoramic dorsal view of the dorsal brain in Fig. 6A shows four of these cell groups. One group of four rMEp cells (about 12 µm in diameter each) projected neurites

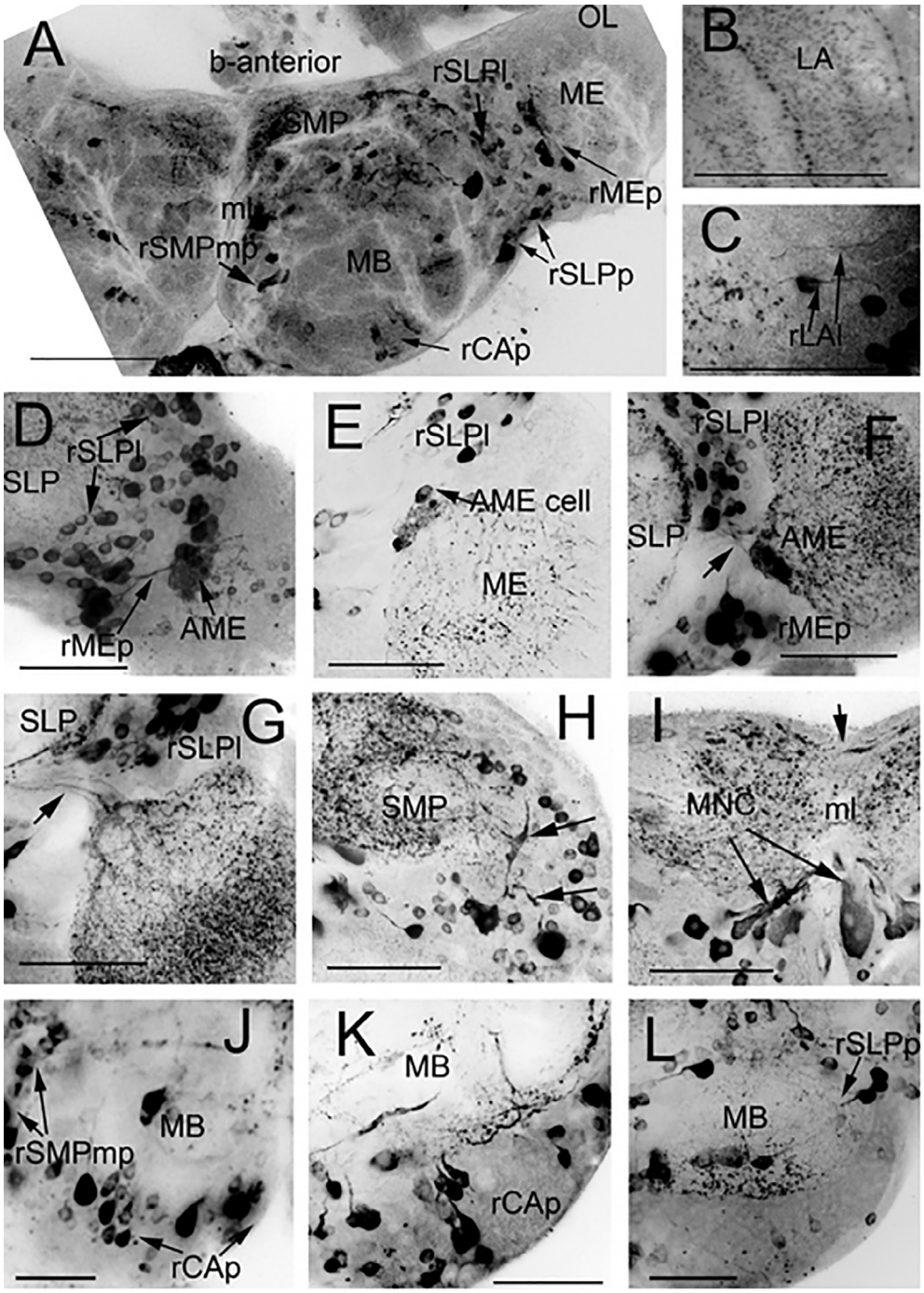

Fig. 8. FLP-IR neurons and their projections. The gray scale is inverted to depict intense fluorescence as black. All images are dorsal views of the brain and OL. A and B are stacks of 34 sections each. C is 1 µm section. D-L are stacks of 5 µm sections each. A. Low magnification of the brain showing the general plan of the ramifications of FLP-IR cells, in the OL the rMEp cells and the rSLPp, rSMPmp and rCAp cells in the PR. B. FLP-IR in the LA C. Enlargement of rLAl cells in LA. D. rMEp cells projecting axons to AME (arrow). E. FLP- IR AME cells juxtaposed to AME (arrow). F-G. FLP-IR neurites pass between the AME and SLP (arrow in F) and numerous rSLPl cells on the lateral edge of SLP. H. Numerous FLP-IR cells and their neurites on the dorsal surface of SLP and SMP. I. FLP-IR in several MNC (arrows). J. rCAp cells and rSMPmp cells (out of focus in image A). K. rCAp axons project anteriorly towards MB. L. rSLPp cells appear to project axons to MB. Scale bars = 50 µm in A-C; 30 µm in D-L.

initially to the ME. A second group of two cells, the rSLPp cells (about 10–12 µm in diameter each), projected neurites medially to the SLP. A third group of 2–3 rSMPa cells (about 8 µm in diameter each) projected intertwined neurites medially to the SMP. A fourth group of about 15 rSMPmp cells (about 10 µm in diameter each) projected neurites anteriorly to the SMP. Details are given below.

Fig. 6B–E shows images from a single series captured at different depths, from the most ventral (Fig. 6B) to the most dorsal (Fig. 6E). The rMEp cells projected neurites mainly to the ME (Fig. 6B; Fig. 7G), but a few branched out to the AME (Fig. 6B, arrow). This preference is shown clearly when anti-PDF was also used to mark the position of the AME (Fig. 7G-I1). In the ME, the rMEp neurites arborized extensively (Fig. 6B–D) and emerge in one of two directions: some project distally to ME and then to the LA (Fig. 6G). Others emerge from the proximal side of the ME and project to the LO, either directly (Fig. 6C, white arrow) or indirectly via the AME (Fig. 6B, C, black arrows). Within the LO, these neurites arborized widely (Fig. 6B–D) and from there, they project medially to the SLP (Fig. 6D). Fig. 6E shows the trajectory of a fascicle of neurites from the ME/AME to the SLP (arrows).

In the SP, neurites from the rSLPlp cells (Fig. 6E), rSMPa cells (Fig. 6A) and rSMPmp cells (Fig. 6H), and probably neurites from rMEp cells, all enriched a broad web of arborizations mainly on the dorsal surface of the SLP and the SMP (see Fig. 6A; Fig. 7J-L1). Neurites from the rSMPmp cells arborized also in the MB (Fig. 6H). Many 5HT-IR neurites cross the ml, probably providing a means of communication between the two brain hemispheres (Fig. 6I, arrows), as do all the other neuron types studied here.

3.6. Association of 5HT-IR cells with clock cells

A brain treated with both anti-5HT and anti-PDF is shown in the panoramic images in Fig. 7A–C, showing two areas of possible interactions between projections from 5HT-IR cells and clock neuron projections in the merged image in Fig. 7B. Box 'a' indicates the area of the optic lobe and is shown in detail in the enlarged images in Fig. 7D-L1. Box 'b' indicates the PPA area and is shown in detail in the enlarged images in Fig. 7M-O1.

Fig. 7D–F shows that the AME is strongly fluorescent with PDF-IR neurites from the LNs (Fig. 7F), but only faintly fluorescent with very fine 5HT-IR neurites, which lack varicosities (Fig. 7D). No convincing superimpositions were seen in the merged image in Fig. 7E. More dorsal images from the same series (Fig. 7G-I1) show both the 5HT-IR rMEp (Fig. 7G) and the LNs (Fig. 7I). The merged image in Fig. 7H, and the enlargement of the box in it (Fig. 7I1), show numerous points of superposition between 5HT-IR varicosities and PDF-IR varicosities in the ME. The 5HT-IR rMEp neurites show additional superpositions with LN neurites in LA (Fig. 7J-L1). These findings show that the ME and the LA, and to a much lesser extent the AME, are the potential areas of communication between 5HT-IR rMEp cells and LNs. In the area of the PPA (Fig. 7M-O1), neurites fluorescent for both antibodies are seen, but there is no evidence of close associations between them (see enlargement of box in Fig. 7N shown in Fig. 7O1). The absence of such points may relate to the fact that the main area of dense 5HT-IR neurites lies on the dorsal surface of the SMP, whereas the majority of PDF-IR neurites lie in the dorsal surface of the SLP. Thus, it is again clear that the primary area of superposition with the LNs is in the ME.

3.7. FLP-IR cells

FLP-IR was seen in a very large number of cells dispersed throughout the SP and the OL, as shown in the panoramic view of a brain in Fig. 8A. This abundance of FLP-IR cells made it difficult to trace

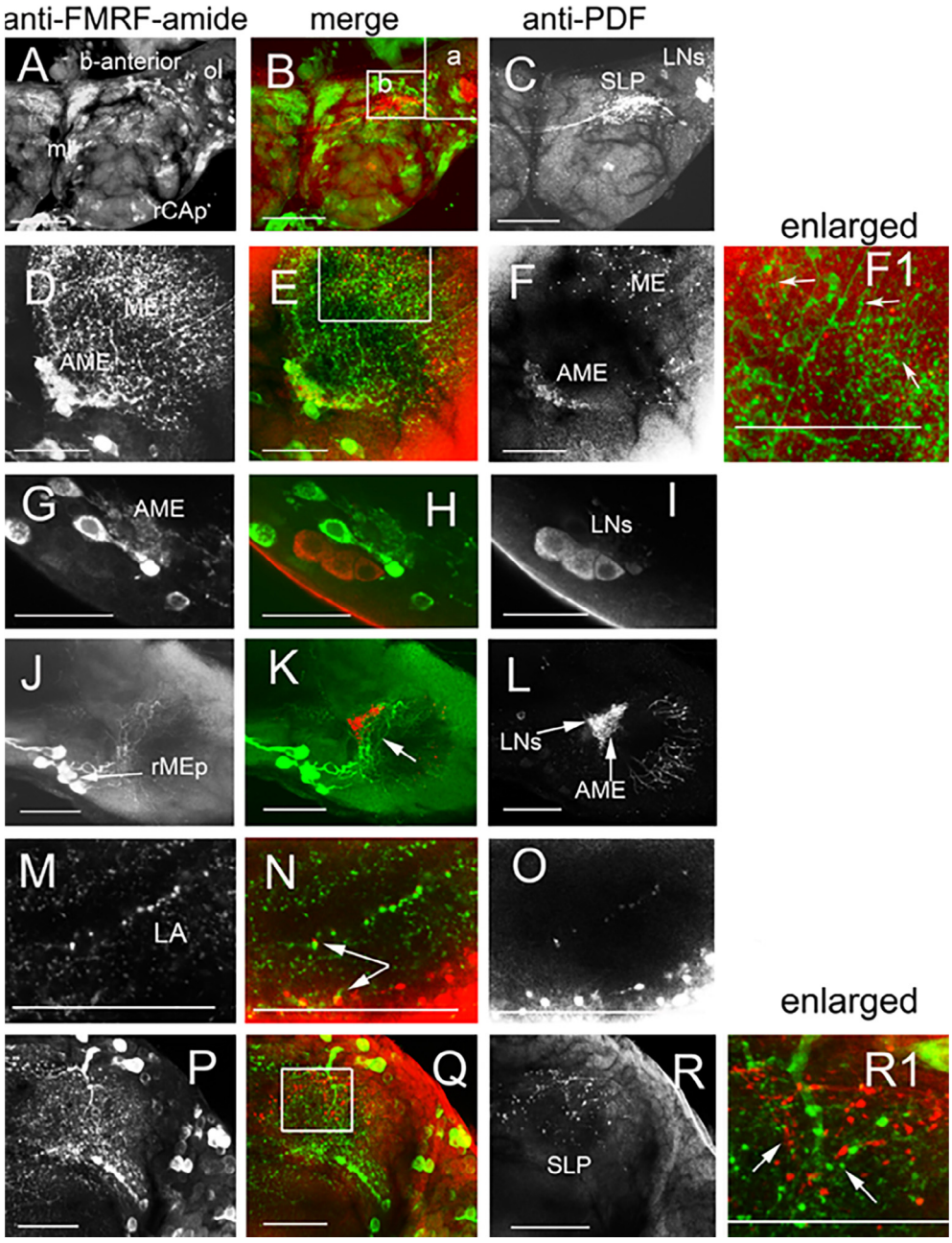

Fig. 9. FLP-IR neurons and neurites (left column, green) related to PDF-IR neurons and neurites from LNs (right column, red). Merged images of left and right are shown in the merge column. Tight superimposition of these two neuron types shows as orange/yellow. All images are dorsal views of the PR and OL. A-C is a stack of 37 sections. D-I and M-R1 are 1 μm sections. J-L is a stack of 5 sections. A-C. Panoramic view of brain showing the OL, LNs and rCAp cells. White-boxed area 'a' is the OL area and enlarged in D-O; area 'b' is the SP and enlarged in P-R1. D-F1. The AME and ME with FLP-IR varicosities sparsely present in AME but abundant in ME, where they are close to PDF-IR varicosities seen in F1, which is enlargement of the box in E. G-I. FLP-IR cells adjacent to LNs. J-L. rMEp cells project axons to both AME and ME, as shown in K. M-O. Sparse associations of the two neuron types in LA. P-R1. No tight superimpositions in SLP, but varicosities of both types are in proximity, seen in RI which is enlargement of the box in Q. Scale bars = 50 μm in A-C; 30 μm in D-R1.

individual neurites. However, there were several distinct areas where their projections were discernible. Two areas were seen in the OL. One area was at the distal end of the OL, where numerous small rLAl cells (Fig. 8C) projected neurites to the LA (Fig. 8B). These cells are similar in location, morphology and size to the CCAP-IR rLAl cells and could be the same cells, but this could not be tested because both antisera to CCAP and FMRFamide were produced in rabbits. The neurites of rLAl cells probably travel to the ME, as was described for CCAP in Section 3.3.

The second area consists of a cluster of about 20 cells (about 6–8 μm in diameter) of FLP-IR rMEp cells arranged in a broad swath. Some of their neurites project to the AME (Fig. 8D, arrow), while others project to the ME, as treatment with both anti-FMRFamide and anti-PDF showed (Fig. 9J–L); FLP-IR neurites in the ME are shown in Fig. 9K (arrow). Most of the rMEp cells are located at a distance from the AME (Fig. 8D). However, 2–3 cells are juxtaposed closely to the dorsal side of the AME, which are named here FLP-IR AME cells (Fig. 8E, arrow). Despite their proximity to the AME, these FLP-IR AME cells have no visible connections with LNs, as treatment with both anti-FMRFamide and anti-PDF shows (Fig. 9G–I). The numerous neurites of all these rMEp cells, the AME cells and probably the rLAl cells, contribute to the extensive network of FLP-IR neurites seen in both the AME (Fig. 9D–F) and in the ME (Fig. 8E–G). From the AME, many neurites projected proximally to the SLP, thus forming a bridge that connects these two parts of the brain as shown in Fig. 8F and G (arrows) and less clearly in Fig. 8D. Whether neurites from the rMEp cells and the AME cells innervate the LA is not clear.

In the lateral dorsal surface of the SLP numerous FLP-IR cells were located (rSLPl cells) in an arch and aligned in rows (clearly shown in Fig. 8D and F and less clearly in Fig. 8G), which projected fluorescent neurites to the SLP where they arborized widely (Fig. 8H) and probably travelled beyond the SLP to much of the SP. Numerous other FLP-IR cells were located on the dorsal surface of the SMP (Fig. 8H, arrows) and projected their neurites into the SMP. Interestingly, many of the MNC are also FLP-IR (Fig. 8I). Along the middle line, a large number of small FLP-IR cells, the rSMPmp cells, were seen; these project neurites anteriorly, towards the SMP (Fig. 8J, arrows). Thus, all the above cells, and possibly FLP-IR neurites from the rMEp cells, form a vast web of arborizations with varicosities in the SP (Figs. 8A, H; 9P), as well as from countless other cells, which reside in other regions of the anterior SP and at various depths, but are not described here. Many FLP-IR neurites cross the ml, again potentially providing a system of communication between contralateral brain hemispheres (Fig. 8I, short arrow).

In the posterior cell body rind posterior to the MB calyx, a large number of FLP-IR rCAp cells of various sizes (6–10 μm in diameter) were seen which reside in an arch formation that neighbors the rSMPmp cells (Fig. 8J, K); they project neurites into the MB (Fig. 8K). Fig. 8L shows that FLP-IR rSLPp cells also project to the MB.

3.8. Association of FLP-IR cells with clock cells

Areas of potential interactions with the LNs were examined using antisera to both anti-FMRFamide (green channel) and anti-PDF (red channel), as shown in Fig. 9. The merged image in Fig. 9B outlines two areas of potential interactions, one in the optic lobe where the LNs are located (area ‘a’) and the second in SP where the PPA is located (area ‘b’).

Area ‘a’ is enlarged in Fig. 9D–O. Fig. 9D-F1 focuses on the ME and the AME area. The merged image in Fig. 9E, shows both the AME and the ME are richly fluorescent with FLP-IR neurites and varicosities. In the enlarged image Fig. 9F1 (arrows) of the box in Fig. 9E, many varicosities were seen close to PDF-IR varicosities but no obvious superposition was seen. Close proximity without clear superposition could indicate communication between LNs and FLP-IP cells over a greater distance, such as by neuromodulation. This possibility also exists in the LA where proximity but sparse superimposition points were seen (Fig. 9M–O; arrows in Fig. 9N). Fig. 9G-I and Fig. 9J-L were described in Section 3.7.

Fig. 9P-R1 is an enlarged image of area ‘b’ in Fig. 9B, where both FLP-IR neurites (Fig. 9P) and PDF-IR neurites from the LNs (Fig. 9R) branch extensively. The enlargement in Fig. 9R1 of the box in Fig. 9Q, shows numerous PDF-IR varicosities closely apposed to FLP-IR varicosities, but as with their proximities in the ME and the AME, no unambiguous superimposition was apparent.

4. Discussion

4.1. Cells of the eye

The widespread distribution of AstA-IR in the brain of various insects and especially in areas related to the circadian clock has implied involvement of this peptide in the circadian system of insects (review by Nässel, 2002). AstA peptides are primarily known for their inhibition of juvenile hormone by the corpora allata but are also considered as brain/gut peptides with myotropic functions on visceral tissues and also regulate feeding and nutrition (e.g. Sarkar et al., 2003; Schoofs et al., 2017; Sedra et al., 2015; reviews by Verlinden et al., 2015).

The neural pathway(s) of entrainment of the circadian clock in the brain of *R. prolixus* has not been studied. Here, we report that in *R. prolixus* AstA cells appear to be central components that relay light information to the LNs, and therefore likely represent a critical pathway for entrainment of the circadian system. We showed that each *R. prolixus* ommatidium possesses a single elongated cell that is strongly IR to anti-AstA-7. Each cell gives rise to a strongly stained long axon which projects through the LA to terminate in the ME. These cells seem to represent either R7 or R8 retinula cells. The AstA-IR neurites of these cells are therefore the initial relays of optic input to the LA and ME, where close superpositions occur with the laterally projecting neurites of the LN clock cells. This arrangement suggests that photic information may be conveyed directly to the circadian system in these neuropils, by AstA acting as a neurotransmitter or neuromodulator. However, we have reported extensive mingling of other neuron types **(**Section 4.2**)** in these neuropils, indicating that extensive processing of photic input occurs here also, and consequently processed aspects of photic information may also be conveyed to the circadian system in these neuropils.

In the Madeira cockroach *Rhyparobia maderae* (previously *Leucophaea maderae*) (Petri et al., 1995) and also in *Schistocerca gregaria* (Würden and Homberg, 1995), AstA-IR cells were restricted to the vicinity of the AME and penetrated the AME. The AstA-IR neurites in *R. prolixus* were not seen to emerge from the ME and did not penetrate the AME. No ASTA-IR cells bodies were seen in the vicinity of the AME or the rest of the OL. We conclude that ASTA-IR cells in *R. prolixus* form initial steps in the photic input pathway and potentially connect with the circadian system in the LA and ME, but not in the AME.

In the ommatidia of a related Triatomid bug, *Triatoma infestans*, daily changes in the migration of pigment granules within the retinula cells was noted (Reisenman et al., 2002). The authors suggested that this rhythmic migration of pigment granules in R7/8 appears to be regulated not only by light but also by the circadian clock. The close contacts of LN neurites with R7/8 AstA-IR neurites in ME and LA in *R. prolixus* may also be indicative that these cells not only transmit photic signals to the clock cells but also receive timing information from it.

4.2. Optic lobe cells

Antisera to CCAP, 5HT and FMRFamide revealed several anatomically distinct groups of cells and their neurites in the OL. No cells showed AstA-IR in the OL, in contrast with other insects (e.g. Kreissl et al., 2010; Petri et al., 1995; Würden and Homberg, 1995). Two general anatomical classes of IR neurons were seen, according to their location. One class was distal (rLA1 cells), and the other in the region of

the ME (rMEd cells for CCAP, rMEp cells for 5HT and FMRFamide). The rLA1 cells were strongly fluorescent with both anti-CCAP and anti-FMRFamide and projected neurites to the lateral surface of the LA. Their trajectories were difficult to follow in the LA. They may terminate in the LA or they may continue to the ME. If the latter is the case, these cells are well positioned to communicate with rMEd neurites from other cell types in both the ME and LA. These cells may correspond to the LA cells in *R. maderae*, which stain with anti-FMRFamide and innervate the LA (e.g. Petri et al., 1995**;** review by Soehler et al., 2011), but in *R. prolixus* they are several-fold more numerous than has been described previously. The LA showed abundant superpositions of CCAP-IR neurites with PDF-IR neurites, raising the possibility that some of these CCAP-IR neurites originate from these rLAl cells. The LA possessed fewer superpositions of FLP-IR neurites with PDF-IR neurites, but it is again possible that some of these may be between rLA1 neurites and the PDF-IR neurites, since rLA1 neurites are recognized by both antisera. However, it was unclear if these cells function as inputs or outputs to the clock.

The second class of OL neurons were in the area of the ME (rMEd and rMEp cells) and project primarily into the ME. The cells in these areas are variously CCAP-IR, 5HT-IR or FLP-IR. No AstA-IR cells were seen on the dorsal surface of the OL. The dense AstA-IR in the ME originates from retinula cells (Section 4.1).

CCAP exhibits myotropic activity in many insects (e.g. Donini and Lange, 2002; Suggs et al., 2016) and participates in the expression of the eclosion program (reviews by Gäde and Hoffmann, 2005; Mykles et al., 2010). In the optic lobe of *R. prolixus*, The CCAP-IR rMEd cells project neurites to the ME, where they arborize extensively, and thence to the LA. No projections to the AME were detected. CCAP-IR did not co-localize with PDF-IR cells, in contrast to observations with the PDF cells in *R. maderae* (Petri et al., 1995), *S. gregaria* (Würden and Homberg, 1995) and two cricket species (Sehadová et al., 2003). Many close superpositions of the CCAP-IR neurites were seen with LNs in both the ME and LA suggesting communication between the CCAP cells and clock cells occurs in these neuropils, indicating that CCAP is also part of the circadian system in *R. prolixus*.

5HT has a plethora of functions in insects, including feeding and appetite, insulin signalling, body size, learning memory, sleep, courtship and mating (reviews by Helfrich-Förster, 2018; Vleugels et al., 2015). 5HT is an important component of the circadian system; it induces phase shifts (e.g. Page, 1987, Cymborowski, 2003; Tomioka, 1999; Yuan et al., 2005) and plays a role in the modulation of the insect visual system. In the flies, *Musca domestica* and *D. melanogaster*, the axons of first-order interneurons in the LA, the L1 and L2 cells, undergo circadian cycling in their cross-sectional area that is modulated by 5HT microinjection (Meinertzhagen and Pyza, 1999).

In *R. prolixus,* the four rMEp cells are 5HT-IR. Their neurites have complex projections. Initially, they project to the ME, but a few neurites also enter the AME. They arborize extensively and form varicosities in the ME, but then emerge, some distally to the LA and some proximally to the LO and thence to the SLP. The modest branching in the AME appeared devoid of varicosities. Thus, the 5HT-IR rMEp cells project to *all* of the optic lobe neuropils and then extend into the SLP itself. The complexity of 5HT-IR projections and their extension into the main SLP area invite the suggestion that 5HT-IR cells may be involved in more than modulation of visual input, but also in relaying outputs of the circadian system to areas in the central brain. The role of 5HT in the circadian system appears more complex than is currently recognised.

The FLPs are involved in the regulation of a multitude of physiological activities as neurotransmitters, neuromodulators and neurohormones (references in Introduction). FLPs also play a key role in the circadian system of several insects. Injection of FMRFamide near the AME of *R. maderae* induced phase-shifts of the locomotor rhythm; since several cells that are PDF-IR are also FLP-IR, it was suggested that FLPs may be released from these cells, making it a clock output (review by Soehler et al., 2011). But microinjections of FMRFamide opposed the effects of PDF on circadian cycling in the size in axons of L1 and L2 cells in the LA of flies, suggesting that FLPs act as an input to the circadian system (review by Pyza and Meinertzhagen, 2003).

In *R. prolixus*, some FLP-IR rMEp cells project into the AME but did not noticeably arborize there; other neurites projected to the ME where they arborized and formed many varicosities. A few FLP-IR cells were seen juxtaposed to the AME, in very close proximity to the LNs, but did not appear to enter it. The LNs were not FLP-IR, in contrast to previous reports in *R. maderae* (e.g. Petri et al., 1995; review by Soehler et al., 2011), *S. gregaria* (Würden and Homberg, 1995) and the flies *M. domestica* and *D. melanogaster* (Meinertzhagen and Pyza, 1999), in which PDF-IR co-localized with FLP-IR in several of the clock cells. Our findings agree with the more recent reports in *M. domestica* and *D. melanogaster*, in which neighboring but different cells express either FLP mRNA or PDF mRNA, showing these two neuropeptides are in different cells (Matsushima et al., 2007). A small number of superimpositions with LN neurites was seen in both the ME and LA, but not in the AME, suggesting that the ME and LA are possible areas of communication between FLP-IR cells and clock cells. While it is tempting to speculate that FLPs are functional in the *R. prolixus* circadian system, the low selectivity of the FMRF antiserum the short sequence of FMRFamide betokens caution.

Finally, the presence of fine neurites IR to antisera to CCAP, 5HT or FMRFamide connecting the ME and AME with the SLP emphasises the importance of communication between the OL and the central brain.

4.3. Accessory medulla

In *R. prolixus,* the AME is a proximal appendix of the medulla, as in other species. In other insects, it contains a wide variety of IR transmitters/modulators, and is regarded as the central component of integration in the circadian system (see Section 1). In *R. prolixus*, its complement of IR neurites other than those of the LNs is very sparse and thus not consistent with this established view. No AstA-IR was detected and CCAP-IR and 5HT-IR neurites were both rare. FLP-IR neurites were quite common and a few FLP-IR cell bodies (the AME cells) were seen juxtaposed to the AME, but were not seen to enter it. The AME in *R. prolixus* appears to represent little more than a passage for the dense tangle of neurites of the LNs which pass through it. On emergence from the AME, LN neurites promptly separate into two branches, one projecting distally to the ME and LA, the other projecting centrally to the SP. These three neuropils abound with IR neurites of many, if not all, of the four neuron types studied here. These neuron types were traced to cells in specific locations, almost all in the OL, but not in close proximity to the AME. Evolutionarily, it may be that *R. prolixus* represents an earlier stage in the concentration of neural organization in the AME seen in flies.

4.4. Superior protocerebrum and PPA

An extensive, dense field of PDF-IR neurites from LNs occupies the dorsal surface of the SLP, and some of the SIP and SMP. They exhibit many varicosities and seem to terminate in this area. PDF-IR neurites from both hemispheres were seen here. We named this area the PPA (see Vafopoulou et al., 2010; Vafopoulou and Steel, 2012a,b).

The PPA occupies a vast area of the dorsal protocerebrum, far removed from the LN cell bodies, and is the only area of LN projections beyond the OL. It abounds with fields of neurites that are IR to all of the four antibodies used here, originating from cells in the anterior, lateral and posterior cell body rind and the cell body rind along the ml. These findings encourage the view that the PPA represents terminations of the LNs in which circadian information is distributed to a diversity of nervous output pathways. We have shown that clock cell neurites make intimate associations with the neurites of various neuroendocrine cells in the PPA and seem to drive rhythmicity in their release (Vafopoulou and Steel, 1996a,b, 2002, 2005, 2012; Vafopoulou et al., 2007). Here,

clock cell neurites in the PPA make close superpositions with anti-AstA-7 neurites and anti-CCAP neurites, suggesting roles for these neuron types in mediating outputs in the PPA. In the case of AstA-IR, neurites of the large rSLPp cell (Maximus), and its companion cells, make intimate associations with PDF-IR neurites in the PPA. Since Maximus is probably neurosecretory, AstA may be another neurohormone driven by the clock. Its companion cells, may mediate other down-stream rhythms of the LNs. In *D. melanogaster*, the PLP cells express AstA and are involved in the regulation of feeding and sleep; these cells are in contact with neurites of PDF-expressing lateral clock cells and express functional receptors for PDF (Chen et al., 2016), indicating that PDF modulates the activity of the AstA PLP cells. Thus, it appears that AstA is an output of the *D. melanogaster* clock. The emerging picture is that circadian information is distributed to both endocrine and behavioral rhythms by AstA neurons.

Many of the MNC in *R. prolixus* were stained with anti-FMRFamide, a phenomenon seen before by Tsang and Orchard (1991) using a general FMRFamide antibody. Anti-FMRFamide also stains the MNC in other insects (references in Shiga, 2003). In *R. prolixus*, the insulin-like peptide cells and testis ecdysiotropin cells, both of which release their hormones rhythmically (references in Section 1), are members of the MNC group. It is possible that FLPs play a role in this rhythmicity.

No close superpositions of LN neurites with either FLP-IR or 5HT-IR neurites were seen in the PPA. However, both cell types were abundant and seen in close (but not intimate) proximity to LN neurites. Communication of these cell types to, or from, the LNs could still occur via neuromodulation and/or interneurons.

We found that the ml of the brain is traversed by all four neuron types studied here, in addition to the LNs themselves (Vafopoulou et al., 2010; Vafopoulou and Steel, 2012b), suggesting the possibility that these neurons couple output rhythms in hormone release and/or behavior between the hemispheres. Clearly, integration of left and right hemispheres is complex, necessary and apparent.

The present work also reveals the importance of the posterior protocerebrum to the circadian system. Several neurites from posterior FLP-IR rCAp cells project anteriorly into the MB, which is also penetrated by LN neurites (Vafopoulou et al., 2010; Vafopoulou and Steel, 2012b). Some rCAp cells are CCAP-IR and project to the SMP, where superimposition was seen with LN neurites. Possibly, some rCAP cells are both FLP-IR and CCAP-IR. The significance of these findings lies in the fact that the DN clock cells (Vafopoulou et al., 2010) are also located in the posterior protocerebrum. It is possible that FLP-IR and/or CCAP-IR rCAp neurites also make associations with the neurites of DNs, serving to coordinate the DN and LN clock cells.

5. Conclusions

We have shown that all four cell types studied here possess associations with the known clock cells. These associations in all cases are found in multiple locations. Surprisingly, the AME is sparsely supplied with neurites other than from the LNs themselves; major areas of potential communication to and from the LNs are the ME and PPA, in both of which IR of all four neuron types was seen tightly associated with clock cells. The organization of the ME suggests roles in both entrainment and in outputs from the clock, whereas that of the PPA suggests it is the main area for distribution of clock outputs to both endocrine and behavioral rhythms. The circadian system of the insect brain is vastly more complex than a coupled population of clock cells, for these cells show extensive evidence of a complex web of connections with both inputs and outputs with various other neuron types located in several different neuropils of the brain. This association of the clock system with different neuron types takes place in seven different neuropil regions of the brain of *R. prolixus*: all three OL neuropils (LA, ME, LO) and four protocerebral neuropils (SLP, SIP, SMP, that together house the PPA, and the MB). This spatial separation of associations of the clock cells with other neuron types implies related separation of clock-regulated functions, raising the potential to study the functions of the pathways of which they are part separately from one another. This potential does not arise in insect species in which many pathways appear compressed into a single, structurally complex AME.

Acknowledgments

This work was supported by Discovery Grant 6669 from the Natural Sciences and Engineering Research Council of Canada.

Declaration of Interest

None.

References

Allada, R., Chung, B.Y., 2010. Circadian organization of behavior and physiology in *Drosophila*. Annu. Rev. Physiol. 72, 605–624. https://doi.org/10.1146/annurev-physiol-021909-135815.

Audsley, N., Weaver, R.J., 2009. Neuropeptides associated with the regulation of feeding in insects. Gen. Comp. Endocrinol. 162, 93–104. https://doi.org/10.1016/j.ygcen.2008.08.003.

Blenau, W., Thamm, M., 2011. Distribution of serotonin (5-HT) and its receptors in the insect brain with focus on the mushroom bodies. Lessons from *Drosophila melanogaster* and *Apis mellifera*. Arthropod Struct. Dev. 40, 381e394. https://doi.org/10.1016/j.asd.2011.01.004.

Bloch, G., Hazan, E., Rafaeli, A., 2013. Circadian rhythms and endocrine functions in adult insects. J. Insect Physiol. 56–69. https://doi.org/10.1016/j.jinsphys.2012.10.012.

Cavanaugh, D.J., Geratowski, G.D., Wooltorton, J.R.A., Spaethling, J.M., Hector, C.E., Zheng, X., Johnson, E.C., Eberwine, J.H., Sehgal, A., 2014. Identification of a circadian output circuit for rest:activity rhythms in *Drosophila*. Cell 157, 689–701. https://doi.org/10.1016/j.cell.2014.02.024.

Chen, J., Reiher, W., Hermann-Luibl, C., Sellami, A., Cognigni, P., Kondo, S., Helfrich-Förster, C., Veenstra, J.A., Wegener, C., 2016. Allatostatin A signalling in *Drosophila* regulates feeding and sleep and is modulated by PDF. PLOS Genet. 12 (9), e1006346. https://doi.org/10.1371/journal.pgen.1006346.

Crane, B.R., Young, M.W., 2014. Interactive features of proteins composing eukaryotic circadian clocks. Annu. Rev. Biochem. 83, 191–219. https://doi.org/10.1146/annurev-biochem-060713-035644.

Cymborowski, B., 2003. Effects of 5,7-dihydroxytriptamine (5,7-DHT) on circadian locomotor activity of the blowfly *Calliphora vicina*. J. Insect Sci. 3, 1–8. https://doi.org/10.1673/031.003.1401.

Donini, A., Lange, A.B., 2002. The effects of crustacean cardioactive peptide on locust oviducts are calcium-dependent. Peptides 23, 683–691. https://doi.org/10.1016/S0196-9781(01)00662-3.

Elia, J., TeBrugge, V., Orchard, I., 1993. The pulsatile appearance of FMRFamide-related peptides in the hemolymph and loss of FMRFamide-like immunoreactivity from neurohaemal areas of *Rhodnius prolixus* following a blood meal. J. Insect Physiol. 39, 459–469. https://doi.org/10.1016/0022-1910(93)90077-5.

Ellen, C.W., Mercer, A.R., 2012. Modulatory actions of dopamine and serotonin on insect antennal lobe cells: insights from studies *in vitro*. J. Mol. Hist. 43, 401–404. https://doi.org/10.1007/s10735-012-9401-7.

Gäde, G., Hoffmann, K.H., 2005. Neuropeptides regulating development and reproduction in insects. Physiol. Entomol. 30, 103–121. https://doi.org/10.1111/j.1365-3032.2005.00442.x.

Golombek, D.A., Rosenstein, R.E., 2010. Physiology of circadian entrainment. Physiol. Rev. 90, 1063–1102. https://doi.org/10.1152/physrev.00009.2009.

Helfrich-Förster, C., 2004. The circadian clock in the brain: a structural and functional comparison between mammals and insects. J. Comp Physiol A 190, 601–613. https://doi.org/10.1007/s00359-004-0527-2.

Helfrich-Förster, C., 2009. Neuropeptide PDF plays multiple roles in the circadian clock of *Drosophila melanogaster*. Sleep Biol. Rhythms 7, 130–143. https://doi.org/10.1111/j.1479-8425.2009.00408.x.

Helfrich-Förster, C., 2014. From neurogenetic studies in the fly brain to a concept in circadian biology. J. Neurogen. 28, 329–347. https://doi.org/10.3109/01677063.2014.905556.

Helfrich-Förster, C., 2018. Sleep in Insects. Annu. Rev. Entomol. 63, 69–86A. https://doi.org/10.1146/annurev-ento-020117-043201.

Homberg, U., Reischig, T., Stengl, M., 2003. Neural organization of the circadian system of the cockroach *Leucophaea maderae*. Chronobiol. Int. 20, 577–659. https://doi.org/10.1081/CBI-120022412.

Ito, K., Shinomiya, K., Ito, M., Armstrong, J.D., Boyan, G., Hartenstein, V., Harzsch, S., Heisenberg, M., Homberg, U., Jenett, A., Keshishian, H., Restifo, L.L., Rössler, W., Simpson, J.H., Strausfeld, N.J., Strauss, R., Vosshall, L.B., 2014. A systematic nomenclature for the insect brain. Neuron 81, 755–765. https://doi.org/10.1016/j.neuron.2013.12.017.

Krajniak, K.G., 2013. Invertebrate FMRFamide related peptides. Protein Pept. Lett. 20, 647–670.

Kreissl, S., Strasser, C., Galizia, C.G., 2010. Allatostatin immunoreactivity in the honeybee brain. J. Comp. Neurol. 518, 1391–1417. https://doi.org/10.1002/cne.22343.

Lange, A.B., Orchard, I., Lloyd, R.J., 1988. Immunohistochemical and electrochemical detection of serotonin in the nervous system of the blood feeding bug, *Rhodnius prolixus*. Arch. Insect Biochem. Physiol. 8, 187–201. https://doi.org/10.1002/arch.940080305.

Lee, D.H., Lange, A.B., 2011. Crustacean cardioactive peptide in the Chagas' disease vector, *Rhodnius prolixus*: presence, distribution and physiological effects. Gen. Comp. Endocrinol. 174, 36–43. https://doi.org/10.1016/j.ygcen.2011.08.007.

Lee, D.H., Paluzzi, J.P., Orchard, I., Lange, A.B., 2011. Isolation, cloning and expression of the crustacean cardioactive peptide gene in the Chagas' disease vector *Rhodnius prolixus*. Peptides 32, 475–482. https://doi.org/10.1016/j.peptides.2010.06.035.

Lee, D.H., Taufique, H., Silva, R., Lange, A.B., 2012. An unusual myosuppressin from the blood-feeding bug *Rhodnius prolixus*. J. Exp. Biol. 215, 2088–2095. https://doi.org/10.1242/jeb.067447.

Lee, D.H., Vanden Broeck, J., Lange, A.B., 2013. Identification and expression of the CCAP receptor in the Chagas' disease vector, *Rhodnius prolixus*, and its involvement in cardiac control. PLoS One 8:e68897. doi:10.1371/journal.pone.0068897.

Matsushima, A., Takano, K., Yoshida, T., Takeda, Y., Yokotani, S., Shimohigashi, Y., Shimohigashi, M., 2007. Double-labelled *in situ* hybridization reveals the lack of co-localization of mRNAs for the circadian neuropeptide PDF and FMRFamide in brains of the flies *Musca domestica* and *Drosophila melanogaster*. J. Biochem. 141, 867–877. https://doi.org/10.1093/jb/mvm094.

Meelkop, E., Temmerman, L., Schoofs, L., Janssen, T., 2011. Signalling through pigment dispersing hormone-like peptides in invertebrates. Prog. Neurobiol. 93, 125–147. https://doi.org/10.1016/j.pneurobio.2010.10.004.

Meinertzhagen, I.A., Pyza, E., 1999. Neurotransmitter regulation of circadian structural changes in the fly's visual system. Microsc. Res. Tech. 45, 96–105 10.1002/(SICI)1097-0029(19990415)45:2 < 96::AID-JEMT4 > 3.0.CO;2-L.

Mykles, D.L., Adams, M.E., Gäde, G., Lange, A.B., Marco, H.G., Orchard, I., 2010. Neuropeptide action in insects and crustaceans. Physiol. Biochem. Zool. 83, 836–846. https://doi.org/10.1086/648470.

Nässel, D.R., 2002. Neuropeptides in the nervous system of *Drosophila* and other insects: multiple roles as neuromodulators and neurohormones. Prog. Neurobiol. 68, 1–84.

Nässel, D.R., Winther, A.M.E., 2010. *Drosophila* neuropeptides in regulation of physiology and behavior. Prog. Neurobiol. 92, 42–104. https://doi.org/10.1016/j.pneurobio.2010.04.010.

Numata, H., Miyazaki, Y., Ikeno, T., 2015. Common features in diverse insect clocks. Zool. Lett. 1, 10. https://doi.org/10.1186/s40851-014-0003-y.

Ons, S., Richter, F., Urlaub, H., Pomar, R.R., 2009. The neuropeptidome of *Rhodnius prolixus* brain. Proteomics 9, 788–792. https://doi.org/10.1002/pmic.200800499.

Orchard, I., 2006. Serotonin: A coordinator of feeding-related physiological events in the blood-gorging bug, *Rhodnius prolixus*. Comp. Biochem. Physiol. A 144, 316–324. https://doi.org/10.1016/j.cbpa.2005.11.010.

Page, T.L., 1982. Transplantation of the cockroach circadian pacemaker. Science 216, 73–75. https://doi.org/10.1126/science.216.4541.73.

Page, T., 1987. Serotonin phase-shifts the circadian rhythm of locomotor activity in the cockroach. J. Biol. Rhythms 2, 23–34. https://doi.org/10.1177/074873048700200103.

Paluzzi, J-P.V., Bhatt, G., Wang, G.H., Zandawala, J.M., Lange, A.B., Orchard, I., 2015. Identification, functional characterization, and pharmacological profile of a serotonin type-2b receptor in the medically important insect *Rhodnius prolixus*. Front. Neurosci. 9, 175. https://doi.org/10.3389/fnins.2015.00175.

Petri, B., Stengl, M., Würden, S., Homberg, U., 1995. Immunocytochemical characterization of the accessory medulla in the cockroach *Leucophaea maderae*. Cell Tissue Res. 282, 3–19. https://doi.org/10.1007/s004410050454.

Pittendrigh, C.S., 1993. Temporal organization: reflections of a Darwinian clock-watcher. Annu. Rev. Physiol. 55, 16–54. https://doi.org/10.1146/annurev.ph.55.030193.000313.

Pyza, E., Meinertzhagen, I.A., 2003. The regulation of circadian rhythms in the fly's visual system: involvement of FMRFamide-like neuropeptides and their relationship to pigment dispersing factor in *Musca domestica* and *Drosophila melanogaster*. Neuropeptides 37, 277–289. https://doi.org/10.1016/j.npep.2003.06.001.

Reischig, T., Stengl, M., 2003. Ultrastructure of pigment-dispersing hormone-immunoreactive cells in a three-dimensional model of the accessory medulla of the cockroach *Leucophaea maderae*. Cell Tissue Res. 314, 421–435. https://doi.org/10.1007/s00441-003-0772-7.

Reisenman, C.E., Insausti, T.C., Lazzari, C.R., 2002. Light-induced and circadian changes in the compound eye of the haematophagous bug *Triatoma infestans* (Hemiptera: Reduviidae). J. Exp. Biol. 205, 201–210.

Sarkar, N.R.S., Tobe, Stephen S., S.S., Orchard, I., 2003. The distribution and effects of Dippu-allatostatin-like peptides in the blood-feeding bug *Rhodnius prolixus*. Peptides 24, 1553–1562. https://doi.org/10.1016/j.peptides.2003.07.015.

Schoofs, L., De Loof, A., Van Hiel, M.B., 2017. Neuropeptides as regulators of behavior in insects. Annu. Rev. Entomol. 62, 35–52. https://doi.org/10.1146/annurev-ento-031616-035500.

Sedra, L., Lange, A.B., 2014. The female reproductive system of the kissing bug, *Rhodnius prolixus*: arrangements of muscles, distribution and myoactivity of two endogenous FMRFamide-like peptides. Peptides 53, 140–147. https://doi.org/10.1016/j.peptides.2013.04.003.

Sedra, L., Lange, A.B., 2016. Cloning and expression of long neuropeptide F and the role of FMRFamide-like peptides in regulating egg production in the Chagas vector*Rhodnius prolixus*. Peptides 82, 1–11. https://doi.org/10.1016/j.peptides.2016.05.003.

Sedra, L., Haddad, A., Lange, A.B., 2015. Myoinhibitors controlling oviduct contraction within the female blood-gorging insect *Rhodnius prolixus*. Gen. Comp. Endocrinol. 15 (211), 62–68. https://doi.org/10.1016/j.ygcen.2014.11.019.

Sehadová, H., Sauman, I., Sehnal, F., et al., 2003. Immunocytochemical distribution of pigment-dispersing hormone in the cephalic ganglia of polyneopteran insects. Cell Tissue Res. 312, 113–125. https://doi.org/10.1007/s00441-003-0705-5.

Selcho, M., Millán, C., Palacios-Muñoz, A., Ruf, F., Ubill, L., Chen, J., Bergmann, G., Ito, C., Silva, V., Wegener, C., Ewer, J., 2017. Central and peripheral clocks are coupled by a neuropeptide pathway in *Drosophila*. Nat. Commun. 8, 15563. https://doi.org/10.1038/ncomms15563.

Shiga, S., 2003. Anatomy and function of brain neurosecretory cells in Diptera. Microscopy Res. Technique 62, 114–131. https://doi.org/10.1002/jemt.10366.

Singaravel, M., Fujisawa, Y., Hisada, M., Saifullah, A.S.M., Tomioka, K., 2003. Phase shifts of the circadian locomotor rhythm induced by pigment-dispersing factor in the cricket *Gryllus bimaculatus*. Zool. Sci. 20, 1347–1354. https://doi.org/10.2108/zsj.20.1347.

Soehler, S., Stengl, M., Reischig, T., 2011. Circadian pacemaker coupling by multi-peptidergic cells in the cockroach *Leucophaea maderae*. Cell Tissue Res. 343, 559–577. https://doi.org/10.1007/s00441-010-1091-4.

Sokolove, P.G., 1975. Localization of the cockroach optic lobe circadian pace-maker with microlesions. Brain Res. 87, 13–21. https://doi.org/10.1016/0006-8993(75)90775-1.

Stangier, J., Hilbich, C., Beyreuther, K., Keller, R., 1987. Unusual cardioactive peptide (CCAP) from pericardial organs of the shore crab *Carcinus maenas*. Proc. Natl. Acad. Sci. U.S.A. 84, 575–579. https://doi.org/10.1073/pnas.84.2.575.

Stay, B., Chan, K.K., Woodhead, A.P., 1992. Allatostatin-immunoreactive cells projecting to the corpora allata of adult *Diploptera punctata*. Cell Tissue Res. 270 (15), 23. https://doi.org/10.1007/BF00381875.

Stengl, M., Arendt, A., 2016. Peptidergic circadian clock circuits in the Madeira cockroach. Curr. Opin. Neurobiol. 41, 44–52. https://doi.org/10.1016/j.conb.2016.07.010.

Suggs, J.M., Jones, T.H., Murphree, S.C., Hillyer, J.F., 2016. CCAP and FMRFamide-like peptides accelerate the contraction rate of the antennal accessory pulsatile organs (auxiliary hearts) of mosquitoes. J. Exp. Biol. 219, 2388–2395. https://doi.org/10.1242/jeb.141655.

Taghert, P.H., Nitabach, M.N., 2012. Peptide neuromodulation in invertebrate model systems. Neuron 76, 82–97. https://doi.org/10.1016/j.neuron.2012.08.035.

Tomioka, K., 1999. Light and serotonin phase-shift the circadian clock of the cricket optic lobe *in vitro*. J. Comp. Physiol. A 185, 437–444. https://doi.org/10.1007/s003590050404.

Tomioka, K., 2014. Chronobiology of crickets: a review. Zool. Sci. 32, 624–632. https://doi.org/10.2108/zs140024.

Tsang, P.W., Orchard, I., 1991. Distribution of FMRFamide-related peptides in the blood-feeding bug *Rhodnius prolixus*. J. Comp. Neurol. 311, 17–32. https://doi.org/10.1002/cne.903110103.

Uryu, O., Ameku, T., Niwa, R., 2015. Recent progress in understanding the role of ecdysteroids in adult insects: Germline development and circadian clock in the fruit fly *Drosophila melanogaster*. Zool. Lett. 1, 32. https://doi.org/10.1186/s40851-015-0031-2.

Vafopoulou, X., Steel, C.G.H., 1996b. Circadian regulation of a daily rhythm of release of prothoracicotropic hormone from the brain-retrocerebral complex of *Rhodnius prolixus* (Hemiptera) during larval-adult development. Gen. Comp. Endocrinol. 102, 123–129. https://doi.org/10.1006/gcen.1996.0053.

Vafopoulou, X., Steel, C.G.H., 1996a. The insect neuropeptide prothoracicotropic hormone is released with a daily rhythm: re-evaluation of its role in development. Proc. Natl. Acad. Sci. U.S.A. 93, 3368–3372. https://doi.org/10.1073/pnas.93.8.3368.

Vafopoulou, X., Steel, C.G.H., 2002. Prothoracicotropic hormone of *Rhodnius prolixus*: partial characterization and rhythmic release of neuropeptides related to *Bombyx* PTTH and bombyxin. Invertebr. Reprod. Dev. 42, 111–120. https://doi.org/10.1080/07924259.2002.9652767.

Vafopoulou, X., Steel, C.G.H., 2005. Testis ecdysiotropic peptides in *Rhodnius prolixus*: biological activity and distribution in the nervous system and testis. J. Insect Physiol. 51, 1227–1239. https://doi.org/10.1016/j.jinsphys.2005.06.013.

Vafopoulou, X., Steel, C.G.H., 2009. Circadian organization of the endocrine system. In: Gilbert, L.I. (Ed.), Insect Development: Morphogenesis, Molting and Metamorphosis. Academic Press, London, pp. 393–458.

Vafopoulou, X., Steel, C.G.H., 2012a. Insulin-like and testis ecdysiotropin neuropeptides are regulated by the circadian timing system in the brain during larval-adult development in the insect *Rhodnius prolixus* (Hemiptera). Gen. Comp. Endocrinol. 179, 277–288. https://doi.org/10.1016/j.ygcen.2012.08.018.

Vafopoulou, X., Steel, C.G.H., 2012b. Metamorphosis of a clock: remodeling of the circadian timing system in the brain of *Rhodnius prolixus* (Hemiptera) during larval-adult development. J. Comp. Neurol. 520, 1146–1164. https://doi.org/10.1002/cne.22743.

Vafopoulou, X., Steel, C.G.H., 2014. Synergistic induction of the clock protein PERIOD by insulin-like peptide and prothoracicotropic hormone in *Rhodnius prolixus* (Hemiptera): implications for convergence of hormone signaling pathways. Front. Physiol. 19, 5–41. https://doi.org/10.3389/fphys.2014.00041.

Vafopoulou, X., Steel, C.G.H., Terry, K.L., 2007. Neuroanatomical relations of prothoracicotropic hormone cells with the circadian timekeeping system in the brain of larval and adult *Rhodnius prolixus* (Hemiptera). J. Comp. Neurol. 503, 511–524. https://doi.org/10.1002/cne.21393.

Vafopoulou, X., Terry, K.L., Steel, C.G.H., 2010. The circadian timing system in the brain of the fifth larval instar of *Rhodnius prolixus* (Hemiptera). J. Comp. Neurol. 518, 1264–1282. https://doi.org/10.1002/cne.22274.

Vansteensel, M.J., Michel, S., Meijer, J.H., 2008. Organization of neuron and tissue circadian pacemakers: a comparison among species. Brain Res. Rev. 58, 18–47. https://doi.org/10.1016/j.brainresrev.2007.10.009.

Verlinden, H., Gijbels, M., Lismont, E., Lenaerts, C., Vanden Broeck, J., Marchal, E., 2015. The pleiotropic allatoregulatory neuropeptides and their receptors: a mini-review. J.

Insect Physiol. 80, 2–14. https://doi.org/10.1016/j.jinsphys.2015.04.004.
Vleugels, R., Verlinden, H., Vanden Broeck, J., Crane, B.R., Young, Michael W., M.W., 2015. Serotonin, serotonin receptors and their actions in insects. Neurotransmitter 2015 (2), e314. https://doi.org/10.14800/nt.314.
Wei, H., el Jundi, B., Homberg, U., Stengl, M., 2010. Implementation of pigment-dispersing factor-immunoreactive cells in a standardized atlas of the brain of the cockroach *Leucophaea maderae*. J. Comp. Neurol. 518, 4113–4133. https://doi.org/10.1002/cne.22471.
Woodhead, A.P., Stay, B., Seidel, S.L., Khan, M.A., Tobe, S.S., 1989. Primary structure of 4 allatostatins-neuropeptide inhibitors of juvenile hormone synthesis. Proc. Natl. Acad. Sci. U.S.A. 86, 5997–6001. https://doi.org/10.1073/pnas.86.15.5997.
Würden, S., Homberg, U., 1995. Immunocytochemical mapping of serotonin and neuropeptides in the accessory medulla of the locust, *Schistocerca gregaria*. J. Comp. Neurol. 362, 305–319. https://doi.org/10.1002/cne.903620302.
Yoon, J.G., Stay, B., 1995. Immunocytochemical localization of *Diploptera* punctata allatostatin-like peptide in *Drosophila melanogaster*. J. Comp. Neurol. 363, 475–488. https://doi.org/10.1002/cne.903630310.
Yuan, Q., Lin, F., Zheng, X., Sehgal, A., 2005. Serotonin modulates circadian entrainment in *Drosophila*. Neuron 47, 115–127. https://doi.org/10.1016/j.neuron.2005.05.027.
Zandawala, M., Orchard, I., 2015. Identification and functional characterization of FGLamide-related allatostatin receptor in *Rhodnius prolixus*. Insect Biochem. Mol. Biol. 57, 1–10. https://doi.org/10.1016/j.ibmb.2014.12.001.
Zandawala, M., Lytvyn, Y., Taiakina, D., Orchard, I., 2012. Cloning of the cDNA, localization, and physiological effects of FGLamide-related allatostatins in the blood-gorging bug, *Rhodnius prolixus*. Insect Biochem. Mol. Biol. 42, 10–21. https://doi.org/10.1016/j.ibmb.2011.10.002.